Effect of Punching on the Lifetime of Polymer Pipes for the Conveyance of Drinking Water

Mechanics of mAterials for enGineering and Integrity of Structures - MAGIS Paris

2023-2024

Seyedeh Saeideh SAADAT

Seyedeh.saadat@ens-paris-saclay.fr

Reviewer:

Cristian OVALLE RODAS

Supervisors:

Xavier COLIN

Juan Pablo MARQUEZ COSTA

Laboratoire Procédés et Ingénierie en Mécanique et Matériaux (PIMM)

51 Boulevard de l'Hôpital – 75013, Paris, France

Table of Content

NOMENCLATURE

ASTM	American Society for Testing of Materials
TGA	Thermogravimetric analysis
CRB	Cracked Round Bar Test
DSC	Differential Scanning Calorimetry
FEM	Finite Element Method
FEA	Finite Element Analysis
FNCT	Full Notch Creep Test
FTIR	Fourier Transform InfraRed spectroscopy
GPC	Gel Permeation Chromatography
HDPE	High-Density Polyethylene
HOCl	hypochlorous acid
LEFM	Linear Elastic Fracture Mechanics
LDPE	Low-Density Polyethylene
MRS	Minimum Required Strength
MW	Molecular Weight
MWD	Molecular Weight Distribution
NHP	Notched HDPE Pipes
NHR	Notched HDPE Ring
NPT	Notched Pipe Test
OD	Outer Diameter
OIT	Oxidation Induction Time
PE	Polyethylene
PE100-RC	HDPE Resistant to Crack
PENT	Pennsylvania Notch Test
PLs	Point Load
PLT	Point Load Test
PLT+	Accelerated Point Load Test
SCC	Stress Corrosion Cracking
SDR	Standard Dimension Ratio
SCG	Slow Crack Growth

1. Motivation

Among the polymer materials used for fluid transport, High-Density Polyethylene has constituted a significant portion of conduits in drinking water distribution networks since the 1990s. HDPE is the most common pipe material utilized across the world, especially in the production of piping materials. For over half a century this material has been choose for use in drinking water systems due not only to its unique properties, like corrosion resistance, flexibility, light weight, toughness, easy installation, water neutrality and leak tightness, but also to its sufficiently long service lifetime. Since these materials were initially introduced, there has been a substantial improvement in their performance. As far as the durability of polymer pipe and resistance to chlorine for the newest type of HDPE is estimated to be up to 100 years.

Nevertheless, this expectation of the lifetime of polymer pipes, especially PE pipes, is assured only under conditions of internal overpressure with pure distilled water (without chlorinated disinfectants) under pressure. However, we should consider there are other factors, which can reduce lifetime of the pipes.

Thanks to the new generation of HDPE, the conduit made of the last generation of resin has been known for its properties of resistance to PL, PE100-RC, can be installed with trenchless techniques and coarse-grained backfill materials. Consequently, there is a potential risk of the existence of a local inhomogeneous stress field caused by a rock pressing onto the outside wall of a polymer pipe. Therefore, the service life of buried pipes can be significantly reduced due to this punctual load during non-conventional pipe installations. Therefore, with this stress concentration, we regard a premature failure in polymer pipes.

Otherwise, microscopic analyses carried out in various studies and articles have revealed that cracks caused by the effect of PL appear on the internal surface of polymer conduits. This observation raises the question of whether the punching effect is the sole cause of this damage, or whether there is a complex interaction between the mechanical effect of punching and the chemical degradation induced by chlorinated disinfectants, which are commonly used in the treatment of drinking water.

Guaranteeing the reliability of drinking water distribution networks is a significant challenge for public health and the proper functioning of urban infrastructure. Otherwise, every year, large investments are buried in the ground when repairing and extending drinking water networks The aim of our study is to precisely investigate the specific effect of puncturing on the structural properties of polymer pipes used in drinking water systems. This study will help determine to what extent these internal deformations affect the lifetime of the pipes and performance, and assess their potential to lead to system failures. Additionally, it will explore whether the observed damage results solely from puncturing or is influenced by other factors, such as chemical degradation caused by chlorinated disinfectants. Understanding the combined impact of these factors is crucial to better comprehend the mechanisms of degradation and to develop strategies for prevention and improvement.

Although experimental tests accounting for these PL effects are rare due to their complexity and duration, therefore this study focuses on the numerical prediction of PL effects over pipe life and their coupling with oxidative degradation initiated by attack from disinfectants.

2. Bibliography

Introduction

In this section, we cover four subsections. We begin by introducing an overview of HDPE pipe properties, especially with the introduction of the latest HDPE generation, PE100. Next, we explore the impact of different loads on these pipes, especially PLs caused by rack trenchless installation. Additionally, we investigate the chemical degradation of polymer pipes exposed to chlorinated disinfectants commonly used in drinking water treatment. Finally, the section concludes with an examination of lifetime prediction, specifically focusing on the combined influence of punching and chemical degradation in polymer pipes.

2.1. Polyethylene Pipe Properties

PE piping materials consist of a polyethylene polymer with additives like colorants, stabilizers, and antioxidants to enhance properties and protect during manufacturing, storage, and service. Classified as a thermoplastic, PE pipes can be fabricated using heat and pressure, and field joints can be made through thermal melting processes, creating a permanent bond.

PE is also a semi-crystalline polymer, exhibiting ordered molecular structures with substantial portions aligning closely in crystalline regions. This semi-crystalline nature results in a low glass transition temperature (T_g) of approximately -183°K (-90°C), contributing to greater toughness, impact resistance, and resistance to rapid crack propagation [Handbook of PE Pipe, 2008]. The higher degree of crystallinity of a PE the higher the density and the better the chemical resistance. [H. Bromstrup, 2004]

Different Generations of PE Pipes

In the first generation of PE production, the objective was to create long chains, making the material vulnerable to point loading and crack expansion due to the parallel arrangement of the chains. Sensitivity to notches and point loads led to pipe failures, resolved only with the addition of comonomers in second generation PE. These comonomers branched the molecular chains, significantly improving the resistance to crack expansion but still requiring costly sand coating due to the effects of point loading. In the third generation of PE, unlike second-generation, comonomers are directly integrated into the long chains, introducing branching in a more controlled manner. This branching results in substantially enhanced protection against punctual loads [J. Lenz, 2001].

HDPE evolves from the first generation PE32, PE40, through the second generation PE63, PE80, the third generation bimodal PE100, to the latest state-of-the-art PE100 RC. The pipe in PE100-RC has the same characteristics in terms of density and weldability as an ordinary pipe in PE100 resin. They have also the same standard dimensions. The difference is in the material's ability to resist of PL and slow cracking, which is almost 10 times greater and excellent mechanical properties and environmental stress crack resistance [*Z. Xiong, R. Wei, 2012*]. The resistance to crack initiation in PE is associated with its amorphous structure, which includes additional ramifications as shown in Figure.1.[Dossier technique of SUEZ]

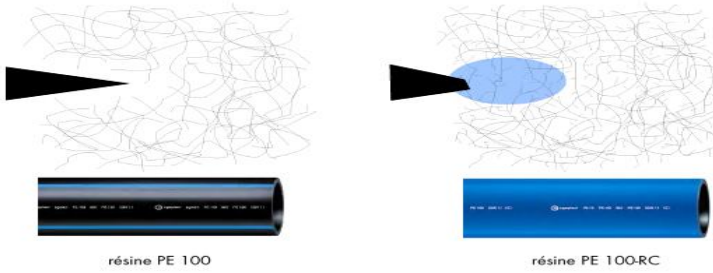

Figure.1. Amorphous structure in different resins of polyethylene

PE100 Properties

PE100, an advanced version compared to the previous generation of PE, is predominantly manufactured using HDPE, resulting in higher density due to increased crystallization. Crystalline PE, with a density of 1.0 g/cm³, contributes to the material's strength, while the amorphous part has a density of 0.85 g/cm³. PE100's enhanced strength is achieved through a higher rate of crystallization, creating a more rigid material with increased density.

The PE100-RC grade of PE, which is a third-generation PE pipe, has been designed, since the end of the twentieth century, to have a bimodal MWD to achieve an optimal balance between strength, ductility, and environmental stress crack resistance. This approach involves a mixture of two molecular sizes, resulting in improved PL resistance and enhanced flexibility in finished pipes compared to traditional single modular PE100 material. The first molecule, similar to monomolecular PE, provides high density, stiffness, and a corresponding high hoop stress value, while the second, more branched molecule, improves notch stress resistance and flexibility. [H. Bromstrup, 2004]

A comparative investigation on two bimodal pipe-grade PE with different PL resistance by Y. Huang, et al., indicates that PE100-RC pipe with better SCG resistance had a stronger deformation recovery capability during stretching [Y. Huang et al., 2020]. Moreover, the Effect of short-chain branches distribution on the fracture behavior of PE pipe resins by [X. He, et al,. 2018] suggest that the chain structure, including MW and its distribution, plays a crucial role in the fracture behavior of PE100-RC [X. He et al. 2018]

Poisson ratio for PE has been found to vary somewhat depending on the ultimate strain that is achieved, on temperature and the density of the base resin. however, for typical working stress, strain and temperature an value between 0.3 to 0.45 is applicable to all PE pipe materials regardless of their densities and also for both short and long-term in-service [Handbook of PE Pipe, 2008].

Toughness, ductility, resilience, and resistance to damage from external loads, vibrations, and pressure surges like water hammer are the inherent properties of the PE pipe. Even in cold weather, they are flexible and can be handled and bent without issue. Based on results from internal pressure tests, the standard extrapolation method outlined in [EN ISO 9080, 2003] categorizes these pipes based on their MRS, ensuring a minimum service life of 50 years. PE 100 is the most recently developed PE grade and PE pipes with higher strength and toughness than earlier generation materials. PE 100 has an MRS of 10.0MPa. [A. Frank et al.2009] To gather information on the resistance to these failure mechanisms, modern methods of LEFM are used. [A. Frank et al.2009]

Young's modulus and yield stress of HDPE can vary based on the supplier and the crystallinity rate of the material. An increase in the crystallinity rate generally leads to an increase in both the elasticity modulus and the yield stress. For PE100, the Young's modulus ranges between 850-1700 MPa, and the yield stress varies between 22-26 MPa according to data sheets.

linear coefficient of thermal expansion for polyethylene varies widely according to different sources. For low-density polyethylene, it is approximately 2 x 10^{-4} °C^{-1} at 20°C, but this coefficient increases to about 3.5 x 10^{-4} °C^{-1} at 80°C. This property is related to the specific volume expansion, which for an isotropic material is three times the linear coefficient. Another reference states a value of 18 x 10^{-4} °C^{-1}. In various technical data sheets from different suppliers, lower values as low as 1.3 x 10^{-4} K^{-1} can also be found.

2.2. BEHAVIOR OF PE PIPES UNDER DIFFERENT MECHANICAL LOADS

The evaluation of PE pipe performance under varying mechanical loads is essential to guarantee the strength and dependability of these piping systems. This section is dedicated to examining how PE pipes respond to two main types of mechanical loads: pressure load and PL.

Hydrostatic Internal Pressure Load

Under static internal pressure, the pipe wall experiences a triaxial stress state, where the most significant stress is the circumferential stress. The axial stress on the inner surface is only half as much as the circumferential stress, while the radial stress corresponds to the internal pressure in the inner surface and on the outer surface, the radial stress is zero.

According to a standard elastic mechanics model, the radial stress (σ_r), circumferential stress (σ_t) and axial stress (σ_a) of a pipe with inner pressure can be calculated according to these formulas:

$$\sigma_r = \frac{P_i\, r_i^2}{r_o^2 - r_i^2}\left(1 - \frac{r_o^2}{r^2}\right) \qquad \textit{Eq.1.}$$

$$\sigma_t = \frac{P_i\, r_i^2}{r_o^2 - r_i^2}\left(1 + \frac{r_o^2}{r^2}\right) \qquad \textit{Eq.2.}$$

$$\sigma_a = \frac{P_i\, r_i^2}{r_o^2 - r_i^2} \qquad \textit{Eq.3.}$$

Where r is the radial coordinate(mm), r_o is the outer radius(mm), r_i is the inner radius(mm) and P_i is the inner pressure (N).

In designing pressure pipes, we follow the normal stress hypothesis, focusing on the highest normal stress, which leads to hoop stress. When a pipe is exposed to internal pressure and the ratio of inside to outside diameter ≤1.3, we specifically consider circumferential stress as:

$$\sigma_{hoop} = \frac{P_i\, D_m}{2e} \qquad \textit{Eq.4.}$$

Where D_m is the average pipe diameter and e is wall thickness (mm). If D_m is replaced by $D_o - e$ dimension formula is:

$$\sigma_{hoop} = \frac{P_i}{10} \cdot \frac{D_o - e}{2e} \qquad \textit{Eq.5.}$$

Where σ_{hoop} is hoop stress or circumferential stress (in N/mm2 or MPa), P = P_i is the inner pressure (bar) and $D_o$is outer diameter of the pipe (mm).

Failure Mechanisms Under Hydrostatic Pressure

The crucial quality of a plastic pressure pipe is its ability to withstand hydrostatic pressure, determining its durability under internal pressure. As mentioned in the previous section, the three-dimensional stress in the pipe wall due to internal pressure is significant. The fracture stress in plastic pipes under internal pressure is influenced by test duration and temperature, extensively studied since 1956. The results are depicted in a log-log graph of test stress against failure time.

The failure mechanisms observed in internally pressurized pipes have been illustrated in the stress-life curve of Figure.2. The relationship between applied load and structural lifetime, reveals three distinct kinetic regimes [A. Frank et al., 2007]. Each of these three parts of the curve corresponds to a different failure mechanism.

In the first regime (**A**), at high stress levels and at relatively short times t_f, the material shows a ductile failure with large-scale plastic deformation and a gradual slope, which depends upon the material's density [H. Bromstrup, 2004]; Usually, plastic pipe systems are designed to operate below this region.

In the transition to the second regime (**B**), the steep part, the intermediate stress range, the curve steepens, shifting from ductile to quassi-brittle failure. In this regime, the failure is characterized by creep crack initiation, creep crack growth, and only small-scale crack tip plasticity. There is a widely accepted understanding that this failure region significantly impacts the lifetime of applications intended for long-term use [N. Brown and X. Lu, 1991,1993]. This knee-point - the transition from the flat to the steep part of the curve - can only be seen for PE 100 materials, if at all, at elevated temperatures and very long testing times (at 80 °C not before 10,000 hours). The verification of the position of these parts of the curves is carried out using three control test points defined in the European standards. [H. Bromstrup, 2004]

In the third regime (**C**), at low stress levels, the curve sharply steepens, indicating predominantly brittle failure which is nearly load independent and is due to chemical aging and degradation of the polymer chains [B. Choi et al.,2009].

In simpler terms, regimes A and B depict "physical aging," while regime C signifies “chemical aging”. Regimes B and C compete with each other. When chemical degradation occurs rapidly enough, regime B completely vanishes. Changes in the molecular structure and morphology of materials, including factors like molecular mass, distribution, branch concentration, and crystallinity, greatly influence crack initiation and PL. Enhanced polymerization processes and controlled adjustments to these material parameters by suppliers have notably improved resistance to these forms of degradation [E.M. Hoang and D. Lowe, 2008; P. Hutar et al., 2013]. Over the long service life of buried pipes spanning several decades, morphological changes can occur, leading to physical aging. However, effective material stabilization can impede molecular degradation and oxidation processes. The type and concentration of stabilizers significantly impact the lifespan of pressurized pipes, particularly in the quasi-brittle and brittle failure regions. Additionally, the concept of local crack tip aging helps explaining the crack growth mechanisms associated with different stabilizer systems [G. Pluvinage and M. Elwany, 2007]

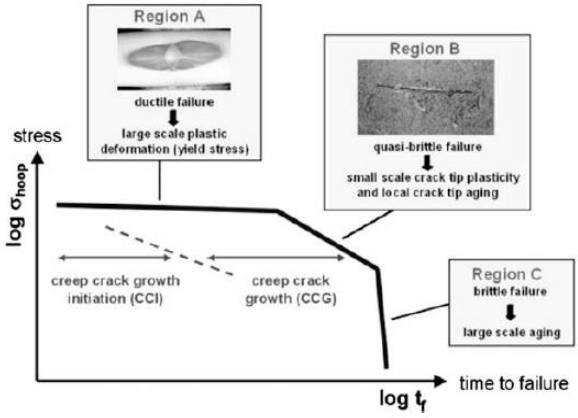

Figure.2. Schematic illustration of the failure behavior of water pressurized PE pipe

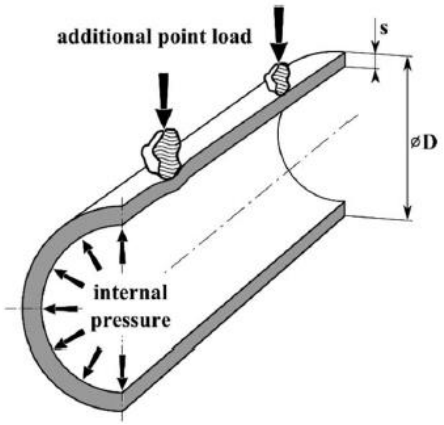

Figure.3. Example of additional PL forces caused by the existence of stone at the external surface of buried pipe.

Point Load

Traditional methods for estimating the residual lifetime of polymer pipes are mainly based on internal pressure tests defined in [EN ISO 9080, 2003] and [ASTM D2837, 2013]. However, these standard procedures reveal limitations, particularly concerning advanced materials like PE 100 or PE 100-RC which don't fail in these standard tests. Therefore, these methods are not sufficient for predicting how long these materials will last.

To address these shortcomings, various accelerated tests like the NPT, PENT, FNCT, and CRB have emerged.[N. Brown and X. Lu,1991; M. Haager,2006] These tests aim at assessing the durability of polymer resins by evaluating their resistance to slow cracking. The majority of articles propose a methodology to estimate the remaining lifetime of polymer pipes. They utilize accelerated tests to measure creep crack propagation and apply fracture mechanics to describe cracks in the pipe wall [P. Hutar et al., 2012; A. Frank et al., 2012]. However, the published articles predominantly concentrate on plastic pipes that undergo only internal pressure testing [P. Hutar et al.,2012; A. Frank et al.,2012; L. Andena et al., 2009, E. Hoang and D. Lowe, 2008; M. Farshad, 2004].

The increased SCG resistance of PE 100-RC presents difficulties for current short-term quality tests, as testing durations for these materials often surpass a year, leading to unacceptable delays and additional problems. For example, in the PENT,

materials no longer develop brittle fractures [A. Sukhadia, 2010] and the detergent Arkopal used for the Cone test [ISO 13480, 1997] and FNCT degrades [F.L. Scholten et al., 2001].

In addition, there is criticism of the often-used FNCT due to the suboptimal sample shape (square instead of round), giving rise to stress singularities. Furthermore, the multiple Round Robins show a large scatter between the different laboratories [U. Niebergall et al., 2006], especially for long testing times.

Furthermore, as the usage of trenchless installation method for polymer pipe is increasing the influence of surface damage on the technical lifetime is becoming more and more important. So many testes have been designed for investigation of the influence of PL on the lifespan of the polymer pipe.

There is therefore a need for new, quick and relevant tests. These have been found in the PL Test, used to determine the pipe quality under point loading.

Point Load Test

Point loads are additional external loads concentrated on a small surface area. A schematic of additional PL forces caused by the existence of stone at the external surface of buried pipes, is shown in Figure.3. The PL Test was developed to investigate the effect of this type of load, specifically to replicate the SCG failure caused by a rock pressing into an external wall of polymer pipes, particularly in cases involving sand-less embedding of pipes for installation [*PAS1075, 2009;* 4 *J. Hessel, 2001*]. The test is described in the standard [PAS 1075, 2009]. This test assesses the resistance of PE materials to such damage, with PE100-RC being a high SCG-resistant PE developed for these applications. It is anticipated to exceed a year in the PLT test. Additionally, an accelerated PLT+ test involving enhanced detergents and higher temperatures has been introduced, with a minimum test duration of 450 hours for a PE100-RC rating [S. Nestelberger, J. Cheng, 2021].

Failure Mechanisms Under Point Loads

Buried pipes, including PE pipes, can experience undesired external forces, such as point loading, originating from rocks in the soil or backfilling material. When a concentrated force is applied to the surface of the pipe, it creates localized stress on the pipe wall at the point of contact. This load leads to permanent local stresses or deformations on the pipe wall. These additional stresses and deformations combine with the pressure-induced tensile stresses inside the pipe. The combined effect of external point loading and internal pressure-induced tensile stresses can reduce the lifetime of buried pipelines, leading to the initiation of cracks.

These cracks may start forming on the inner pipe wall, particularly near the area where the pipe is impacted by rocks. Once initiated, it propagates from the inner side to the outer side of the pipe wall. The propagation of cracks is influenced by the stress concentration at the point of loading and the material's response to these stresses. The propagation of cracks may result in the formation of multiple macroscopic longitudinal lips along the pipe axis. These lips represent sections where the pipe material has fractured, creating visible deformations along the length of the pipe.

The failure mechanism observed in these situations is described as brittle, indicating a lack of macro-ductility. This means that the material does not undergo significant plastic deformation before failure, and the crack propagation is characterized by a more instantaneous and brittle process. This suggests that the failure mode is similar to the PL process, often characterized by a brittle mode of failure. This brittle mode is prevalent in low-pressure, long-term pipeline service operations. [S. Nestelberger, J. Cheng, 2021; V. Rouyer and M. Cornette, 2001; J. lenz, 2001]

The studies highlight the ongoing debate regarding the dominant mechanism in buried pipes subjected to point loading is stress relaxation or constant deformation. Some authors suggest that in stiff types of soil, the governing process is stress relaxation, indicating that pipes are more or less in a situation of constant deformation. On the contrary, other groups assume a constant stress scenario, leading to a creep phenomenon. [V. Rouyer and M. Cornette, 2001]

The nature of the soil and the interaction with the buried pipe are still controversial topics. Different researchers have varying perspectives on whether stress relaxation or constant deformation is the dominant mechanism, likely influenced by the specific properties of the backfilling materials and the surrounding soil. [V. Rouyer and M. Cornette, 2001]

Morphology of Cracks

To improve the understanding of the failure process, Figure.4. illustrates the inner wall and outer wall of the different generation pipes during a PL test. When a dent presses into a PE pipe, it creates a dent on the outside and a bulge on the inside of the pipe. As mentioned, the bulge on the inside leads to additional tensile stresses on the inner wall, in addition to those caused by the internal pressure of the medium. The accumulation of tensile stresses, particularly at the bulge, can lead to premature brittle fractures in the axial direction. The analyses of the crack in Figure 12-G shows that yielding occurs at

the center of the indentation, making the PE stronger due to molecular orientation. However, cracks initiate just next to the center where no yielding occurs, forming a circle around the indentation. From the macroscopic cracking, the multiple cracks around the indentation are described as brittle at the macro scale.

In laboratory testing PL, multiple cracking is observed due to very high-stress levels, whereas in practical applications, only a single axial crack is typically observed. This difference suggests a need for improvement in testing methods to better simulate real-world scenarios. [E. van der Stok and F. Scholten, 2014]

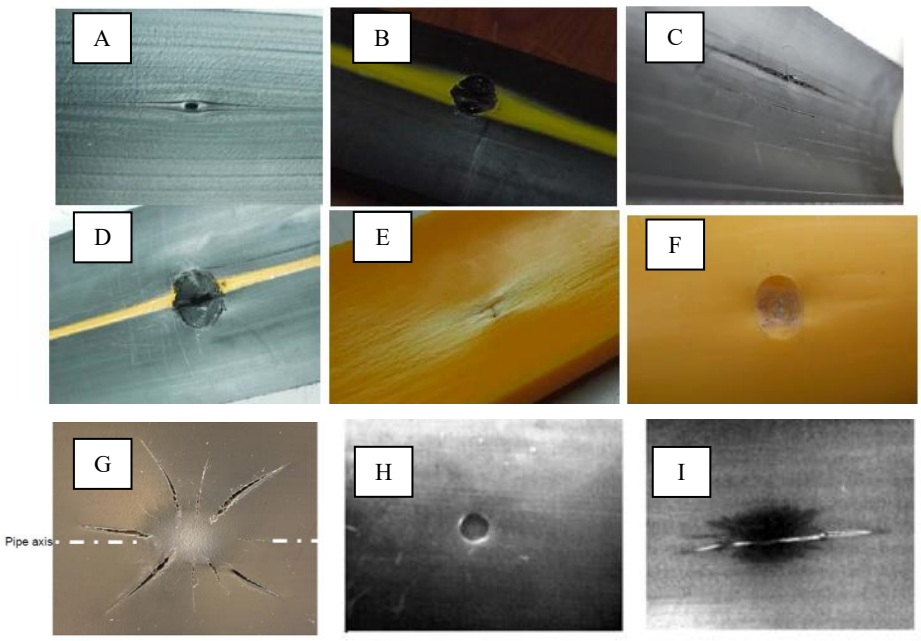

Figure.4. Photograph of the HDPE pipes after PLT
A- B, C-D and E- F) inner wall surface and the outer wall surface around the indentation for PE 80, PE 100 and PE100-RC
*G) for second generation PE pipe after PLT at 80℃ and 8 mm indentation in Dehyton show multiple cracking. The crack starts just next to the center of the indentation where no yielding occurs[*E. *van der Stok and F. Scholten, 2014]*
H and I) stamp on the outside of the PE 100 pipe and crack on the inner wall under the location of the stamp [J. Lenz, 2001]

Effect of Various Parameters on The Point Load on The Lifetime of HDPE Pipes

The rocks can range in size and form, from small sharp-edged stones to large smooth pebbles, to account for the diverse range of rocks encountered in trenchless installations, different kinds of stamps have been used for point loading measurements in the various researches.

Shape of Dentation

A few studies have examined the impact of dent geometries on the failure behaviors of polymer pipes. [Hutař et al., 2011].

[X. Zheng et al., 2019] present a novel approach using a notched HDPE ring specimen to assess the mechanical properties of traditional notched HDPE pipes. Findings highlight reduced ultimate loads with increased notch depth ratio, notably in U-type and V-type grooves compared to L-type grooves. Additionally, the study suggests the potential substitution of NHP specimens with NHR ones for mechanical property testing when the depth ratio is below 0.4 for different groove shapes. The proposed finite element simulation and theoretical model successfully predict ultimate loads, aligning well with experimental results obtained from tension tests.

Dimensions of Dentition

The modification of the stamp diameter exhibits that the stamp size has a crucial influence on the penetration depth [J. Lenz, 2001]. Study shows the penetration depth is smaller with a smaller stamp diameter than a larger one. While the penetration depth did not even achieve 0.1 mm after 10 h with a small stamp diameter. The effects of the PL are higher with a bigger

stamp [J. Lenz, 2001]. the dent introduces additional tension stress on the inner pipe fibers and compression stress on the outer area of the dent. The degree of curvature in the dent directly influences the magnitude of these additional stresses. As the dent becomes greater, the added stress intensifies. When you add radially acting compression stress, it forms an axial compression stress state. Higher compressive loads mean higher reference stress and deeper stamp penetration. The curves reflect this interaction between PL, dent, and resulting stresses [J. Lenz, 2001].

Outer Diameter

Different types of pipe failures, longitudinal, circumferential, or helicoidal, are determined mainly by the pipe diameter. In small diameter pipes, where bending stresses are dominant, failures often manifest circumferentially. Conversely, in large diameter pipes, hoop stresses take precedence over bending stresses, resulting in longitudinal failure. If both bending and hoop stresses are equally significant, the fracture path takes on a spiraled pattern [G. Pluvinage and M. Elwany, 2007]. This phenomenon is observed even when the pipe is under hydrostatic pressure. Consequently, this prompts the question of whether varying pipe sizes could influence stress distribution and loading conditions during the PLT.

with regard to the experimental results, it is evident that various pipe sizes exhibit unique deformation states when subjected to a PL [S. Nestelberger, J. Cheng, 2021]. By maintaining the depth of the dent at a consistent 10% of the pipe wall thickness, there is an escalation in stress intensity with an increase in pipe diameter. The higher stress intensity in larger diameter pipes results in a quicker occurrence of SCG failure compared to smaller diameter pipes [Z. Zho and D. Chang, 2010]

Inner Pressure

The PL test was conducted with different hoop stress by varying water pressure between 1.5 MPa and 4.6 MPa. The results illustrate a reduction in hoop stress corresponds to an increase in failure time. Reducing the internal pressure in the pipelines in practice makes them less prone to failure due to point loading and helps extend the pipeline's lifetime We can also see that decreasing the pressure by a factor of 2 (e.g., from 4 MPa to 2 MPa) extends the pipe's life by approximately 2.5 to 3 times. [E. van der Stok and F. Scholten, 2014]

2.3. CHEMICAL DEGRADATION ASSESSMENT: EFFECTS OF CHLORINE DISINFECTION

PE contains antioxidants, such as phenols, which can react with radicals. This suggests that disinfectants might compromise the durability of PE pipes by destabilizing them, evident in the faster consumption of stabilizers, especially at the water-polymer interface. This reveals how disinfectants could impact the stability of the pipes, potentially raising durability concerns. These chemical reactions alter the material's microstructure, which leads to property degradation and subsequently causes the change of the failure mode.

These alterations, primarily attributed to oxidative degradation, include the formation of carbonyl groups, chain scission, increased crystallinity, and variations in melting temperature. Subsequently, we will explore how these alterations can influence mechanical properties.

Antioxidant Concentration Profiles

Antioxidants play an essential role in keeping safe polymers, like HDPE pipes, against degradation from environmental factors such as oxidation. However, exposure to a chlorine medium, like chlorinated water or water containing chlorine dioxide, significantly reduces the concentration of antioxidants, impacting both stability and mechanical properties [J. Hassinen et al., 2004]. Chlorine dioxide seems to initiate an aggressive attack on antioxidants near the inner wall, employing a single electron transfer process. This process extends deeper into the pipe, continually depleting antioxidants. The chemical consumption surpasses 80% at the inner wall, indicating a substantial loss of stabilizer efficiency. [J. Hassinen et al., 2004]

The decline in antioxidant concentration makes the polymer more susceptible to degradation, especially from oxidative damage. This vulnerability alters the fracture behavior of the material. Weakened sections, particularly those closer to the inner wall, are more prone to crack propagation. As a result, the mechanical strength of the material decreases, making it more brittle and less resistant to stresses and pressures, potentially causing ruptures or fractures. This heightened susceptibility may lead to structural failure even under normal operational stresses. When comparing the effects of chlorinated water versus chlorine dioxide, the latter exhibits a notably faster rate of antioxidant consumption approximately four times faster than chlorinated water [W. Yu et al. 2011]. This accelerated depletion further exacerbates the material's vulnerability to oxidative damage, compromising its structural integrity and mechanical robustness.

Changes in Molecular Weight

Exposure of PE to chlorinated water can significantly impact its MW and distribution. Experimental results reveal that PE oxidation is initiated in the presence of chlorine disinfectant. One primary aspect of this process involves the buildup of hydroperoxides which triggers chain scissions when their concentration is above a critical threshold. Reducing the length of the polymer chains through chain scission results in a decline in the average MW and changes its distribution. This decrease can lead to embrittlement, particularly when Mw gets close to approximately 70 kg /mol. Essentially, these changes in MW can significantly affect properties such as thermal stability, ultimately impacting the performance and lifetime of PE pipes in service. [X. Colin et al., 2009] By Employing Saito relationship, the number of chain scissions s and crosslink events x per mass unit can be calculated from Mn and Mw variations.

$$\frac{1}{M_w} - \frac{1}{M_{w0}} = \frac{s}{2} - 2x \qquad \textit{Eq.7.}$$

$$\frac{1}{M_n} - \frac{1}{M_{n0}} = s - x \qquad \textit{Eq.8.}$$

The competition between crosslink events and chain scissions during PE pipe exposure time is illustrated in Figure.5 [X. Colin et al., 2007].

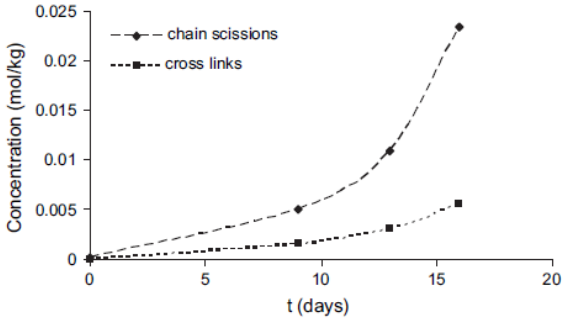

Figure.5. The number of chain scissions and crosslink events per mass unit calculated from the Saito equation against exposure time by Colin et al

Crystallinity Profiles

The degradation of PE through chain scission leads to a decrease in its MW. The shorter chains can more easily incorporate into the crystalline phase of the material, resulting in an increased crystallinity rate during aging. This phenomenon is known as chemi-crystallization. At the nanometric scale, it is characterized by a reduction in the thickness of the amorphous phase located between the crystalline lamellae. These microstructure modifications consequently contribute to the embrittlement of the sample. This increase in crystallinity was measured by differential scanning calorimetry. Figure.6. illustrates the changes in the crystallinity ratio with the changes in the MW.

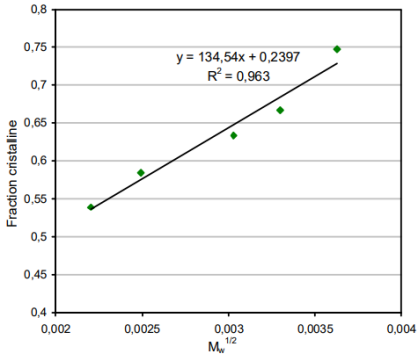

Figure.6. Crystallinity ration as a function of $M_w^{-1/2}$ for PE

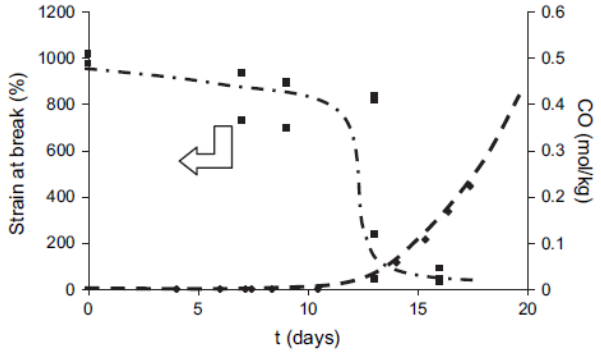

Fig.7. Changes in the ultimate strain ε_R (■) and the concentration of carbonyl groups (♦) during the exposure of PE at 80℃

Influence on Mechanical Behavior

Chemical shifts, like increased carbonyl groups and chain scissions in consequence of changing in molecular mass, reduce the material's strength and ductility. Physical alterations, such as changes in crystallinity (change in morphology) and melting temperature, impact flexibility and thermal stability [A. Frank et al.2009]. Both of these certainly have an effect on the mechanical properties of the pipes and on its resistance to crack initiation and SCG.

The failure mechanism of HDPE moves from a ductile to a brittle mode as the corrosion level increases. This leads to subcritical crack propagation, which deteriorates the load capacity of the structure. Field observations and pressure testing have demonstrated that exposure to chlorinated water leads to premature brittle fractures in PE pipes. [J. Dear and N. Mason, 2001; J. Sanders et al., 2009]

[B. Fayolle et al., 2007]. demonstrated that, in PE strain at break decreases with carbonyl buildup, as shown in Figure.7., illustrating strain at break against exposure time at 80 °C, including the kinetic curve of carbonyl buildup. The observation is that embrittlement, signified by a catastrophic decrease in strain at break, occurs when the carbonyl concentration approaches 0.1 mol kg^{-1}.

Upon comparing Figure 17 and 18, it is evident that carbonyl concentration aligns with the growth in the number of chain scissions and crosslink events, suggesting a correlation between the magnitude of carbonyl concentration and the number of chain scissions, as observed in earlier studies [B. Fayolle et al, 2007]

Fractography

Figure 9 [W. Yu et al., 2011] shows crack that was formed during hydrostatic pressure testing of a pipe exposed to water containing chlorine dioxide. Around the major crack, there are areas of brittle material indicated by the presence of small cracks. These probably indicate parts of the material that are highly degraded. Interestingly, the primary crack advanced into a region of fresh material but ceased further propagation. Then, some aggressive chemicals attacked the material near the crack, suggesting the potential for continued crack growth.

This mechanism, we can name "degradation-assisted crack propagation", explains the possible causes for premature fractures in even thick-walled pipes, even if only the surface of the material is affected by degradation. Figure10 illustrates the different phases involved in degradation-assisted crack growth, providing a visual representation of this phenomenon [W. Yu et al., 2011].

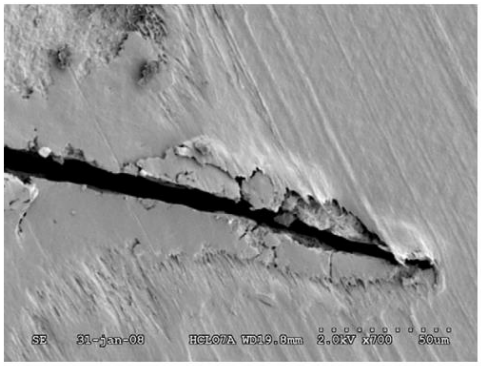

Figure.9. Scanning electron micrograph of a crack in a pipe after 121h of exposure to water containing 4ppm chlorine dioxide.

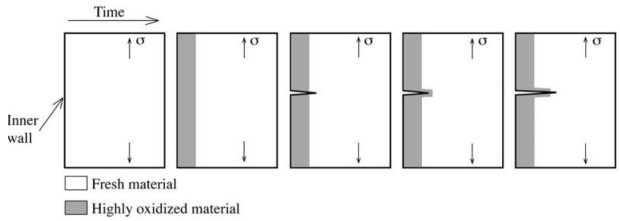

Figure .10. Schematic representation of degradation assists crack propagation. The arrows indicate the principal stress direction

2.4. LIFETIME PREDICTION: COMBINED INFLUENCE OF PUNCHING AND CHEMICAL DEGRADATION

The study of the combined influence of mechanical stress and chemical degradation on the lifetime of polymer pipes represents a critical unexplored area within the current scientific literature. Particularly, there is a notable absence of prior research addressing the combined effect of chlorinated water exposure and point loading on the assessment of polymer pipe durability, signifying a substantial gap in existing knowledge.

In terms of empirical findings, there hasn't been much information about how mechanical and chemical factors work together to influence the lifetime of polymer pipes. However, [A. Tripathi et al., 2021] took a different approach by using a computer model to predict this combined impact. They employed a coupled chemo-mechanical modeling approach to simulate stress

corrosion cracking in HDPE exposed to a bleach solution. The coupled chemo-mechanical model is implemented in a finite element simulation using ABAQUS.

The model introduces a simplified corrosion model, specifically focusing on tracking the diffusion and reaction of HOCl. Application of the model to predict the behavior of HDPE specimens exposed to a corrosive environment under continuous loading produces stress-life curves, As shown in Figure.11. The simulations reveal two distinct regimes for unexposed specimens and three regimes for exposed ones, demonstrating the response of material to different stress levels and corrosion effects. Notably, in the high-stress regime, corrosion has a negligible impact on failure, with yielding dominating. Conversely, in the low-stress regime, corrosion becomes a significant factor, leading to failure through craze breakdown.

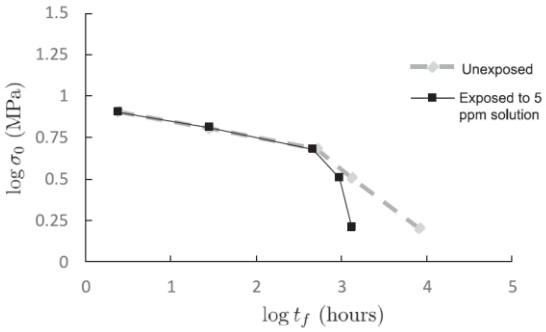

Figure.11. Simulated stress-life curves.

In this model, the fracture kinetics of HDPE have been predicted under different bleach concentrations, offering a comprehensive understanding of crack growth rates. The dependency of crack growth rate on bleach concentration is characterized by two regimes: a constant rate influenced by corrosion and a power-law model representing mechanical loading. The outcomes of this research show that this predictive model emerges as a valuable tool for estimating the service lifetime of HDPE structures. It uniquely considers the interplay between chemical exposure and mechanical stress, addressing the essential aspects overlooked by existing studies.

It is important to note that they simulated a simple tested square rather than a pipe. This approach could limit the reliability of the results in the real world. Additionally, they used HOCl as the chemical species responsible for the degradation, but this cannot be the case since it is not a radical. Instead, it is HO° and Cl° that attack the antioxidants and PE. This constitutes another limitation to consider. The exploration of the combined influence of punching and chemical degradation on polymer pipe lifetime prediction is yet unknown, and it holds practical implications for real-world performance. By doing so, the project seeks to provide a comprehensive understanding of the synergistic effects that these factors may exert on the material properties and structural integrity of polymer pipes.

3. Scientific Approach

3.1. MAIN IDEAS

The central objective of this project is to comprehensively understand the premature failure mechanisms of PE pipes under point loading, exploring the interplay between mechanical stresses and chemical degradation induced by chlorinated disinfectants. This investigation aims to provide insights into how these factors jointly influence pipe failure and develop predictive models for estimating pipe Lifetime.

To achieve this goal, the scientific approach is divided into three phases: 1. examining the impact of punching on mechanical stress and strain distribution within the pipe via the development of finite element software, 2. assessing chemical degradation induced by chlorine disinfection and 3. predicting the pipes' lifetime by considering the combined influences of punching and chemical degradation.

Phase 1: Computational Modelling

In this research phase, we will use the finite element software to create precise models of PE pipes and simulate various PL scenarios accurately. By adjusting factors like the shape and dimensions of the punch, the punching depth, the dimensions of the pipes, and the internal water pressure, we can replicate real-life mechanical pressures on the pipes.

The FEA analysis will compute how stress and strain are distributed within the pipes' structure, particularly focusing on the initiation and propagation of fractures caused by point loading. These findings will offer crucial insights into how well PE

pipes withstand mechanical pressure and will aid in estimating their durability under different stress conditions. Additionally, our parametric analysis enables us to identify critical damage conditions, exploring various parameters to understand the thresholds for damage occurrence. Furthermore, we aim to propose effective solutions aimed at reducing or preventing damage through innovative approaches. This involves damage modeling, seeking to develop comprehensive models that depict the behavior of the pipes under diverse stress situation.

Phase 2: Chemical Degradation Assessment: Effects of Chlorine Disinfection

In the second phase, the project will delve deeper into the effects of chlorinated disinfectants on the stability and longevity of PE pipes. The primary objective is to predict how various levels of chlorination affect PE pipes over time. This will be achieved by observing changes in material properties and degradation mechanisms. This phase involves conducting both physical and chemical characterization tests on materials, as well as assessing mechanical properties at different levels of degradation under chlorine exposure

Phase 3: Lifetime Prediction: Combined Influence of Punching and Chemical Degradation

In the final phase of our research, we will combine the findings from the study of mechanical stresses and chemical degradation to predict the lifetime of PE pipes more accurately. The aim is to understand how mechanical and chemical factors together affect the integrity of the pipes. We will use the data from both these analyses to create models that can simulate the combined effects of point loading and chemical exposure over time. We will also study how continuous chemical attack affects the material properties of the PE pipes when they are subjected to mechanical point loading.

A multi-Physical Problem Solving by solving for the interaction between chemical and mechanical degradation will be carried out to identify which factors most significantly reduce the pipes' service life and under what conditions. The predictive model developed will aim to forecast the point of failure more accurately, allowing for early interventions to improve pipe durability and reliability.

3.2. THE TOOLS AND THE TECHNIQUES

In this section, we will describe the analytical equipment and protocols used for each phase. I will detail also the technical tools employed.

Phase 1: Computational Modelling

For modeling our scenario, Abaqus/CAE 2022 teaching version was used to examine the stress/strain situation in the pipe wall during PLT. The objective is to create accurate models that can investigate the stress/strain distribution in the pipe wall throughout each time step of the loading sequence (punching – heating – internal pressure). Additionally, it enables the calculation of results such as the required force during indentation or the resulting wall thickness reduction below the pin.

The methodology is divided into two parts with different steps. Table 1 summarizes the scientific method used in this phase, each focusing on different aspects of the modeling process.

Part 1: Initial Modeling and Validation

Pipes under internal pressure: First, I modeled a general case of pipes under internal pressure (diameter extern 32mm with thickness 2.9mm under 10bar internal pression), creating both 3D and 2D models. To optimize computational time and resources, the models were simplified. Six different cases were created: full pipes, half-pipes, and quarter-pipes, each in both 3D and 2D. The ABAQUS results were then compared with corresponding analytical results (eq. 1), focusing on circumferential stress, as these stresses are more critical than radial or longitudinal stresses. Once this step was validated, another approach was taken to further validate our model.

Pipe under Point Load: In this step, we began by selecting a reference article to guide our modeling efforts. The scenario described in the reference article was modeled to identify optimal parameters for our simulations in Abaqus, such as finding the best options for contact between the pin and pipe. In the article, a pipe diameter of 32 mm, SDR 11, with a punch diameter of 10 mm and depth of punching equals 8% of diameter extern of pipe were simulated. This stage provided a baseline for parameter identification in the simulation with Abaqus. For the material properties, we used the values from the article, but many parameters were not mentioned. Therefore, we searched other articles, handbooks, or data sheets of PE100 pipes to find values that are adequate to reality.

Adding Thermal and Pressure Loads: In the third step, after validating the model of the pipe under point load, thermal and internal pressure loads were applied to the models step by step. Specifically, a temperature of 80°C and an internal pressure of 885 bar (equivalent to 4 MPa hoop stress) were applied.

Elasto-Plastic Modeling: In the absence of specific details on elasto-plastic studies from the reference article, our study focused on exploring various plasticity models available in Abaqus. Understanding how materials transition from elastic to plastic behavior is crucial, and we utilized the Von Mises criterion to define the yield surface, a fundamental aspect in material modeling.

The Von Mises yield surface is a cylinder in principal stress space, defined by the following formula:

$$f\left(\sigma_{ij}, \bar{\varepsilon}^{p}\right) = \sqrt{\frac{1}{2}\left[(\sigma_1 - \sigma_2)^2 + (\sigma_1 - \sigma_3)^2 + (\sigma_2 - \sigma_3)^2\right]} - Y(\bar{\varepsilon}^{p}) = 0 \qquad Eq.9$$

The radius of this cylinder varies with the yield strength, with its axis parallel to the line σ1=σ2=σ3. If the stress state is inside the cylinder (f < 0), the material behaves elastically. If the stress state is on the cylinder surface (f = 0), the material begins to deform plastically. The yield strength $Y(\bar{\varepsilon}^{p})$ can increase during plastic deformation, indicating that Y is a function of the total plastic strain $\bar{\varepsilon}^{p}$.

Abaqus provides several hardening models: isotropic, kinematic, and combined hardening. Each model influences how materials respond under varying loading conditions. Figure.12. illustrates the various hardening models in Abaqus.

- *Isotropic Hardening*: This model assumes uniform hardening in all directions, leading to equal resistance to plastic deformation throughout the material. It simplifies loading and unloading scenarios by maintaining consistency in the material's response.

- *Kinematic Hardening*: More intricate, this model accounts for the movement of the yield surface. It effectively models phenomena such as the Bauschinger effect, where material behavior differs between loading and unloading cycles. This model is particularly suitable for simulations involving cyclic loading conditions.

- *Combined Hardening*: This model combines aspects of isotropic and kinematic hardening, offering a more comprehensive representation of material behavior under complex loading scenarios. It proves beneficial for materials subjected to varied and cyclic loading conditions.

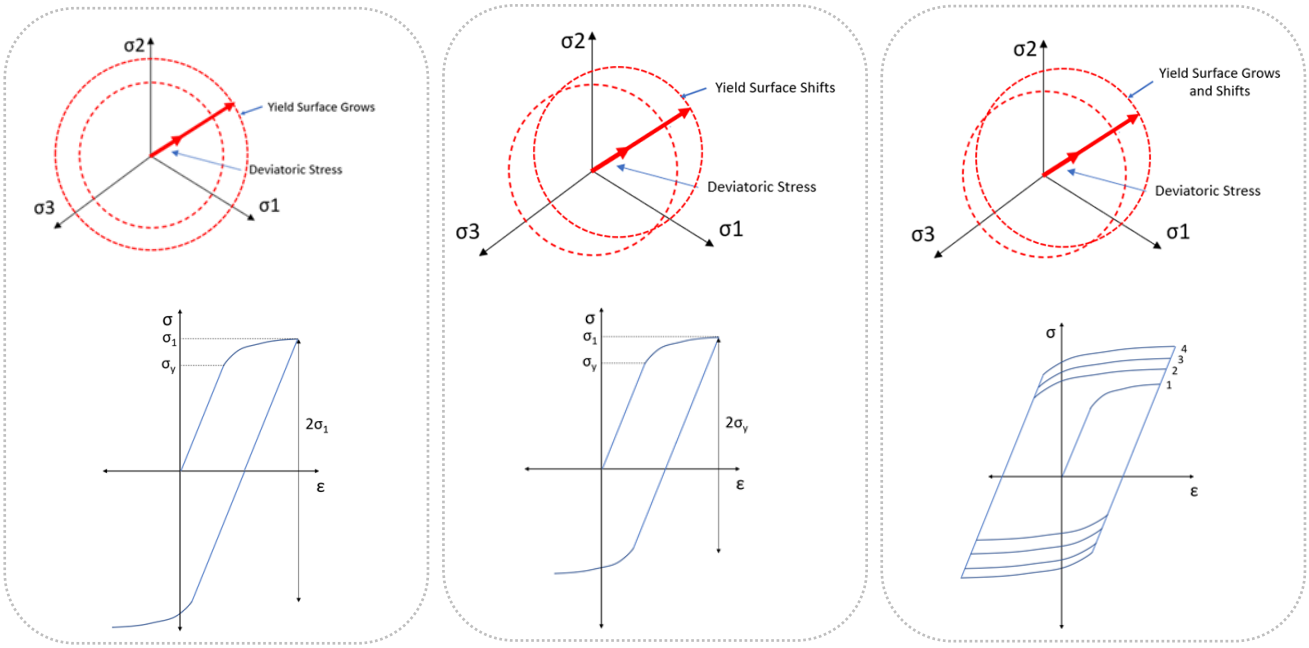

Figure.12. The various hardening models in Abaqus: Isotropic Hardening(left), Kinematic Hardening (middle), Combined Hardening (Right)

Since our model does not involve cyclic loads, we opted for the isotropic hardening model in our simulations. However, we acknowledge that the yield strength may vary with plastic strain. In isotropic hardening, yield strength can be in three forms: perfect plasticity (constant σ_Y), linear strain hardening (σ_Y increases linearly with $\bar{\varepsilon}^{p}$), and power law hardening (where σ_Y follows a power law relationship with $\bar{\varepsilon}^{p}$).

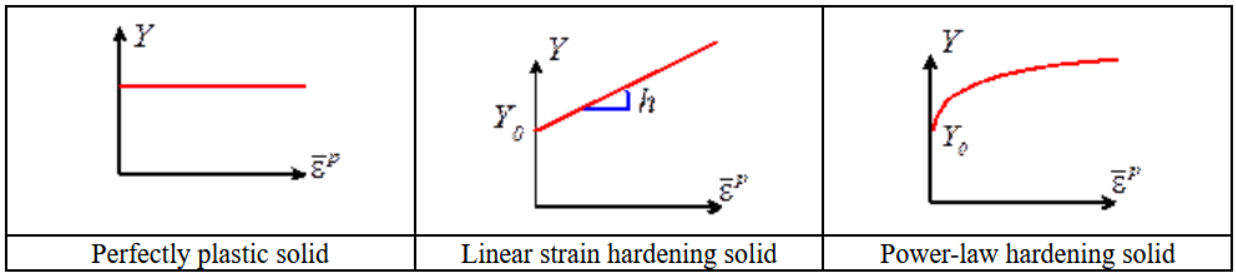

Perfectly plastic solid	Linear strain hardening solid	Power-law hardening solid
$\sigma_Y = constant$	$\sigma_Y\,(\bar{\varepsilon}^p) = Y_0 + h\,\bar{\varepsilon}^p$	$\sigma_Y\,(\bar{\varepsilon}^p) = Y_0 + h\,(\bar{\varepsilon}^p)^{1/m}$

Figure 13. the different form of yield stress

By evaluating these models, we aimed to understand their impact on simulation results and their relevance to real-world material behavior. Our approach underscores the importance of selecting an appropriate hardening model to achieve accurate simulations, ensuring that our results align closely with practical observations and theoretical predictions in material science and engineering.

Step	Description	Parameters	objective
1	General modeling of pipes under internal pressure and comparison of ABAQUS results with analytical results	3D and 2D models of full, half, and quarter pipes; comparison of circumferential stress with analytical results	Optimization of computational resources and validation of model accuracy
2	Modeling specific scenarios based on reference article	Diameter: 32 mm, SDR 11, Punch: 10 mm diameter, 8% depth for PE100	Data retrieval and parameter uncertainty
3	Application of heat and internal pressure	Heat: 80°C, Pressure: 885 bar (4 MPa hoop stress)	Verification against reference results
4	Elastic and elasto-plastic modeling	Different modeled hardening	Matching model parameters with reference data

Table.1. Summery of the method scientific in the first phase

Part 2: reel case and parametric study

Once our model is validated through comparison with reference data, we can proceed to the real case study. We will utilize the same modeling parameters but with different material properties and boundary conditions. Specifically, we will model ¼ of the PE100 pipe with an outer diameter of 90 mm and a wall thickness of 7.8 mm. The pipe will be subjected to a punch with a 10 mm diameter, penetrating to a depth of 8.2% of the pipe's external diameter. The system will be under a pressure of 6 bar at a temperature of 40°C.

The mechanical properties of the PE100 material used in this study are derived from the tensile tests we have conducted. These properties include Young's modulus, yield strength, tensile strength, and elongation at break, which are essential for accurately simulating the pipe's behavior under mechanical stress.

A key objective of this study is to identify critical points where failure is most likely to occur. This involves determining the stress concentrations and analyzing the failure modes of the pipes under purely mechanical loading conditions. By understanding the stress thresholds at which failure becomes imminent, we can gain insights into the material's performance and potential failure mechanism.

Phase 2: Chemical Degradation Assessment: Effects of Chlorine Disinfection

In this phase of the project, we focus on characterizing the materials both before and after degradation due to chlorine exposure. This ensures a comprehensive understanding of material degradation and performance under real-world conditions. To achieve this, a series of tests were initiated to characterize the physical and chemical properties of the materials. Additionally, mechanical tests were conducted to assess the material properties under stress. To analyze changes in the properties of materials at different stages of degradation, we prepared a platform to expose the materials to a chlorine solution

(with a concentration of 4 ppm HoCl at 40°C). Material samples are collected monthly to analyze changes in their properties at different stages of degradation. This phase is divided into three main parts: Film Fabrication Using Compression Molding, Physico-Chemical Characterization of Materials, Mechanical Behavior of Materials.

The material studied

The material used in this study is high density polyethylene, HDPE (PE100) used in the drinking water pipes. It was then extruded to make stoppers. It is a semi-crystalline thermoplastic, comprising an amorphous phase and a crystalline phase, in the form of a spheroidic aggregate. The PE100 grade is one of the latest developments in polyethylene resins, and as a result, guarantees the best mechanical characteristics of all polyethylene resins on the market.

Part 1: Film Fabrication Using Compression Molding

To ensure uniform degradation throughout the material and avoid any gradients, specimens with a thickness of less than 1 mm were prepared. This is crucial for accurately assessing the material properties at various levels of degradation, it was decided to produce a film with a thickness of 600 microns. Consequently, this process was divided into three steps:

Step 1: Characterize materials before film fabrication: Initially, we performed physical and chemical characterization of the materials before starting to fabricate the films under pressure and compression. This was done to determine whether the properties would change after the manufacturing process. For this reason, we have done the ATG, FTIR, OIT, and DSC. we did also the mechanical tensile test the pipes.

Step 2: Fabricate films under various conditions using a compression molding machine: We worked on PE100 pipes so These pipes were cut and ground into small granules suitable for film fabrication using a Gibitre compression molding machine. Our goal was to produce thin films free of defects, with a smooth and flat surface, by varying the conditions of temperature, pressure, and molding time. The following table summarizes the conditions tested:

Film	Temperature	Molding Time	Pressure Time	Cooling Condition
	(°C)	(s)	(s)	
1	160	120	120	Fast
2	160	120	60	Fast
3	160	150	60	Fast
4	160	120	90	Fast
5	160	120	120	Slow
6	180	120	120	Slow
7	180	150	120	Slow

Table.2. Summary of the conditions used in fabrication the films

Step 3: Re-characterize films to assess changes in material properties due to fabrication conditions: After fabricating the films, we repeated the physico-chemical tests (TGA, FTIR, OIT, DSC) to assess any changes in material properties due to the fabrication process. This re-characterization was essential to determine if the material properties had altered under different fabrication conditions.

Finally, we decided to fabricate the films at the temperature of 180°C and waiting 150s for molding the material et after that press the materials under pressure 22 bar for 120s because the films produced under them had a very flat shape without any signification changes in the properties. in additional we have chosen the slow cooling condition because Rapid cooling was found to decrease the degree of crystallinity.

Part 2: Physical-Chemical and Mechanical Behavior characterization before/ after degradation

This section presents the study of the physical-chemical and mechanical characterization of materials before and after degradation. The study is divided into two main steps:

Step 1: Initial Characterization: After fabricating the films, materials without degradation were characterized using the aforementioned tests to establish a baseline.

Step 2: Re-characterization: All characterization tests were then conducted on samples that aged over time. Material samples were collected monthly to analyze changes in their properties at different stages of degradation.

For this purpose, various tests were conducted, including TGA (Thermogravimetric Analysis), FTIR (Fourier Transform Infrared Spectroscopy), OIT (Oxidation Induction Time), DSC (Differential Scanning Calorimetry), and tensile tests. In the following sections, I will explain in detail the methodologies and equipment used for these tests.

Mechanical characterization: uniaxial tensile tests: In order to assess the mechanical properties of the materials, uniaxial tensile tests were systematically conducted. Initially, mechanical tests were performed on samples procured from Suez to establish their baseline mechanical characteristics. The samples underwent precision polishing to achieve the requisite shape for testing. Subsequently, thin specimens were fabricated with a thickness of approximately 6 microns, specifically designed for mechanical evaluation.

Figure 14. Specimens for Tensile Test in Two Thicknesses and the Testing Machine

Following fabrication, tensile tests were performed on these thin specimens' post-degradation to investigate how exposure to chlorine and other degradative factors influenced their mechanical behavior over time. This step aimed to provide insights into the material's durability and performance under simulated environmental stressors.

Given the operational context where pipes are exposed to a 40°C environment, the tensile tests were conducted at this temperature to simulate realistic operating conditions. During testing, specimens were subjected to controlled displacement until failure, with meticulous recording of stress-strain data.

The testing procedures adhered to relevant standards and norms to ensure consistency and reliability of results. Tensile tests were conducted using an Instron 5966 machine equipped with a precision 10 kN load cell. To account for variability, ten tests were performed on samples in their initial state, with an equivalent number conducted on aged samples. The test speeds were meticulously set at 10 mm/min for thicker samples and 5 mm/min for thin films, focusing on assessing both breaking behavior and elastic properties in accordance with ISO 527 standard guidelines.

Thermogravimetric Analysis (TGA): To determine the thermal stability and composition of the materials, we measure weight changes as a function of temperature, including the mass of carbon black. Samples were heated at a controlled rate in an inert atmosphere with two different gas, and weight loss was recorded. In this study TGA of studied samples was carried out using a TA Instruments Q500 analyzer. At first cycle the samples were heated from temperature 30°C to 600°C at a heating rate of 20°C/min under Nitrogen et in the second cycle they were heated from temperature 600°c to 700°C at a heating rate of 20°C/min under oxygen.

FTIR Spectroscopy. To observe changes in a material caused by disinfectant chlorine, HDPE/PE100 was characterized by Fourier transform infrared spectroscopy (ATR FTIR) in the range from 4000 to 650 cm^{-1}. Each sample was pressed with the flat pressure tip at the maximum pressure. From each sample, 8 parallel spectral measurements were carried out. We Identified functional groups and molecular structures present in the materials before and after degradation.

Oxidation Induction Time (OIT): We effected the OIT to measure the oxidative stability of the materials. Samples were heated in a differential scanning calorimeter (DSC) on nitrogen rich environment with flow rate 50 ml/min at first pour arrived a temperature stable et after that we change le gas to the oxygen for a period more than 3h for recording the time to oxidation onset. We conducted at two different temperatures, 220°C and 200°C, with the following conditions for each:

Méthode1:	Method 2:
➢ Selected Gas N2 ➢ Ramp 10°C/min to 220°C ➢ Isotherm 5min ➢ Selected Gas O2 ➢ Isotherm 360min /240min	➢ Selected Gas N2 ➢ Ramp 20°C/min to 200°C ➢ Isotherm 5min ➢ Selected Gas O2 ➢ Isotherm 360min /240min

Table 3. The methodologies used for OIT test

Differential Scanning Calorimetry (DSC): DSC studies were performed on a DSC 25 - TA Instruments (TA Instruments). Samples between 5.0±0.01 et 10.0±0.01 mg were sealed in aluminum pans, heated from 25°C to 220°C at heating rate of 10°C/min. Nitrogen flow rate was 40 ml/min. Measurement of each sample was performed three times. All experiments were carried out under nitrogen atmosphere.

We determined the thermal transitions such as melting and the rate of crystallinity. Samples were heated at a controlled rate, and heat flow was measured to identify thermal events. Rate of crystallinity (χc) was calculated using the formula. where ΔH°f is the enthalpy of fusion for 100% crystalline polyethylene (290 J/g).

$$\chi c = \Delta Hf / \Delta H°f, \qquad Eq\ 10.$$

Phase 3: Lifetime Prediction: Combined Influence of Punching and Chemical Degradation

The third phase of the project aims to predict the lifetime of polyethylene (PE) pipes when subjected to both mechanical punching stresses and chemical degradation. This involves a detailed analysis using experimental data and advanced simulation techniques.

The primary objective of this phase is to quantify how chemical degradation, induced by chlorinated substances, exacerbates the failure of PE pipes under mechanical loading. By understanding the compounded effects of these factors, we aim to elucidate their role in the premature failure of PE pipes.

This advanced approach will simulate the internal layer degradation and its impact on the overall pipe structure when exposed to both mechanical stresses and chemical attacks from chlorinated disinfectant

Methodology

Although Phase 3 has not yet been conducted, the planned approach involves the following steps:

At first, data collected in Phase 2, which includes the physico-chemical characterization and mechanical properties of the degraded materials, will be utilized. This data will help in creating accurate models of degraded PE pipes.

After that, the internal layers of the simulated PE pipe models will be modified to reflect a reduction in mechanical properties due to chemical attack, based on the degradation data obtained from Phase 2. Using ABAQUS, we will dynamically alter the properties of the PE pipe to model real-time degradation effects occurring under service conditions. This involves:

- Establishing Baseline Mechanical Properties: Initial mechanical properties of the PE pipes will be determined.
- Introducing Chemical Degradation Parameters: Chemical degradation parameters will be introduced to simulate the weakening of the material over time.
- Applying Mechanical Loads: Mechanical loads will be applied to observe the interplay between punching stresses and the chemically weakened state of the pipes.

4. Results and discussion

After describing the study material, test protocols, and analysis techniques used, we will now focus on the results of our study, starting with the firs phase of the project.

4.1. PHASE 1: COMPUTATIONAL MODELLING

These simulations allow for precise analysis of the mechanical behavior of the material under various senario. However, accurate results are contingent upon correct model calibration. Therefore, in the initial part of the modelling phase, we verified and validated our model with different approaches. This validation process was divided into four sections, and the following are the results for each part:

Part 1: Initial Modeling and Validation

Pipes under internal pressure: Here, we present the results of the first part of our study, which examines a pipe with an external diameter of 32 mm and a wall thickness of 2.9 mm under an internal pressure of 10 bar. We compare the results from six models of pipes in 2D and 3D configurations (complete pipe, half pipe, and quarter pipe) using Abaqus simulations and analytical calculations based on Equation 5. In the figure.15, we have plotted the circumferential stress distribution from various simulation methods as a function of the distance between the inner and outer radius, as this is the most significant stress in the case of internal pressure.

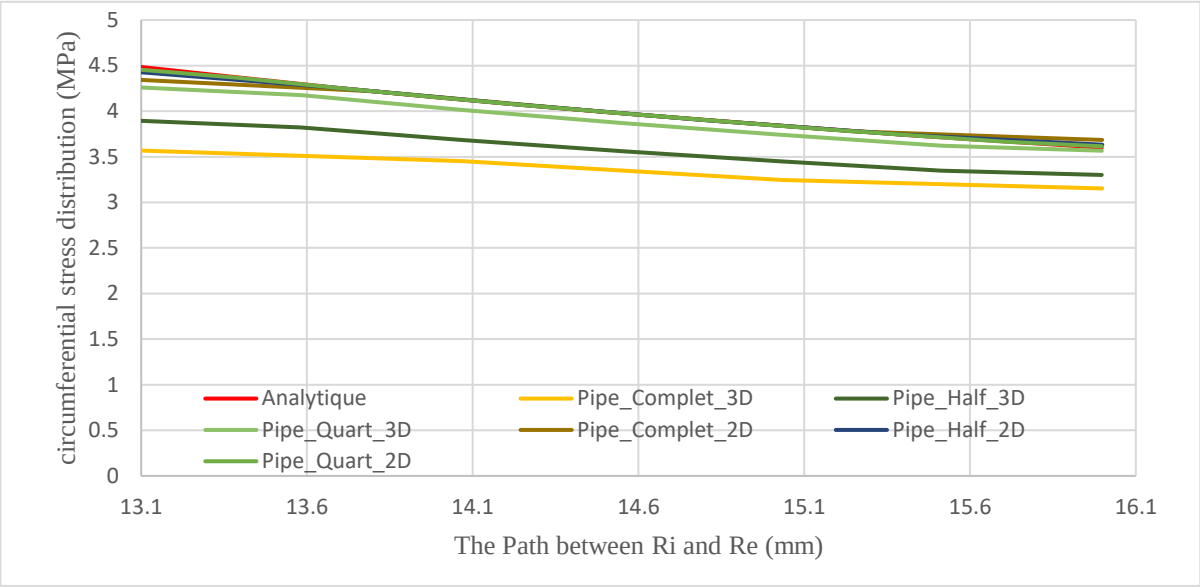

Figure 15. the circumferential stress distribution from various simulation methods

As shown, the results from the 2D simulation exactly match the analytical results. However, there are noticeable differences when comparing the 3D simulation results to both the 2D simulation and the analytical results. This finding underscores the utility of 2D simulations for achieving results that are exactly matched to theoretical predictions that in the specific case of a pipe under internal pressure, simplifying the model from 3D to 2D does not compromise accuracy. The circumferential stress, being the most critical stress under internal pressure, is well captured by the 2D simulations. This simplification significantly reduces computational time and resources while maintaining the fidelity of the results

the discrepancy can be attributed to the limitations of the student version of the software, which restricts the mesh refinement. Consequently, the 3D model exhibits larger deviations. Nevertheless, it is evident that with a highly refined mesh, the 3D simulation results can closely align with the analytical predictions. Additionally, by optimizing the mesh size in 3D simulations, we can achieve results that are nearly identical to those obtained analytically. Therefore, the choice of mesh size is crucial for ensuring accurate simulation outcomes. This study demonstrates that, under the conditions tested, a 3D case can effectively be simplified to a 2D case without altering the results. This simplification is particularly beneficial in practical engineering applications where computational efficiency and resource optimization are paramount.

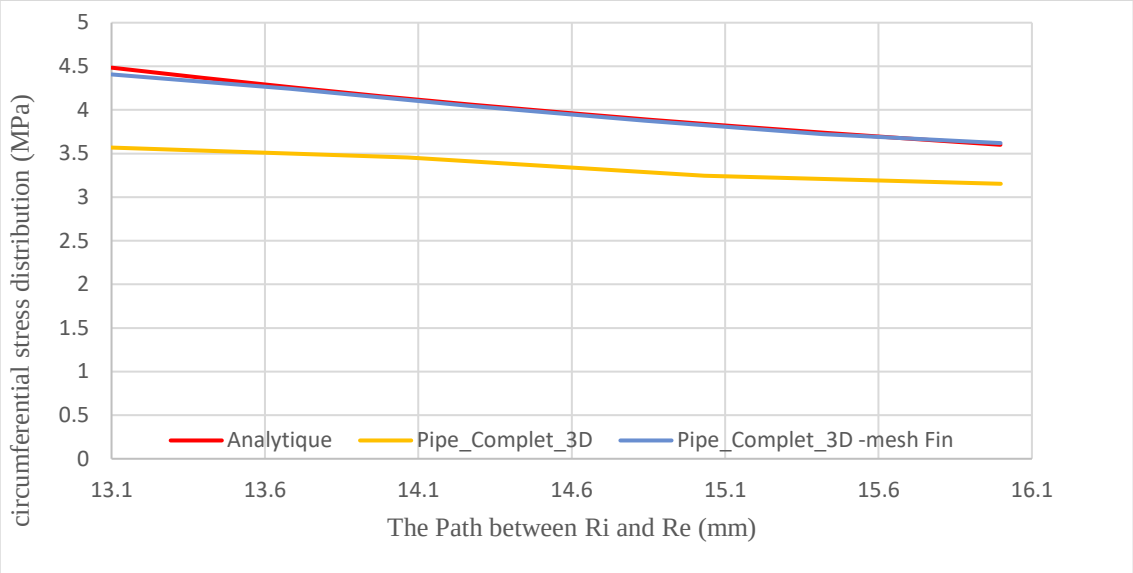

Figure 16. The effect of the mesh size in the resultant.

Pipe under Point Load: In the second part of our study, we modeled a pipe with an outer diameter of 32 mm and a thickness of 2.9 mm subjected to a point load applied by a 10 mm diameter pin, penetrating 8% of the pipe's outer diameter at the contact point. This modeling was conducted in 2D using PE100 material properties: a Young's modulus of 950 MPa and a Poisson's ratio of 0.35, assuming elastic behavior.

Initially, we attempted to simplify the problem by modeling it in 2D. However, we encountered convergence issues when comparing the results with reference values. By switching to a 3D model with the same parameters, we achieved results that aligned more closely with the reference data. This indicated that for point load cases, a 2D model was inadequate. Consequently, we proceeded with 3D modeling for subsequent analyses.

In the 2D model, we experimented with different parameters to approach the reference results, such as the position and shape of the plateau, refining the mesh, and varying the contact parameters between the pin and the pipe, including the coefficient of friction. Despite these adjustments, significant improvements were not observed. Conversely, when modeling the same problem in 3D with identical parameters, the results varied substantially

The circumferential strain distribution under selected loading conditions, as shown in Figure 18., was taken from the inner fiber from the pin to the end cap (indicated by the red arrow in Figure 17).

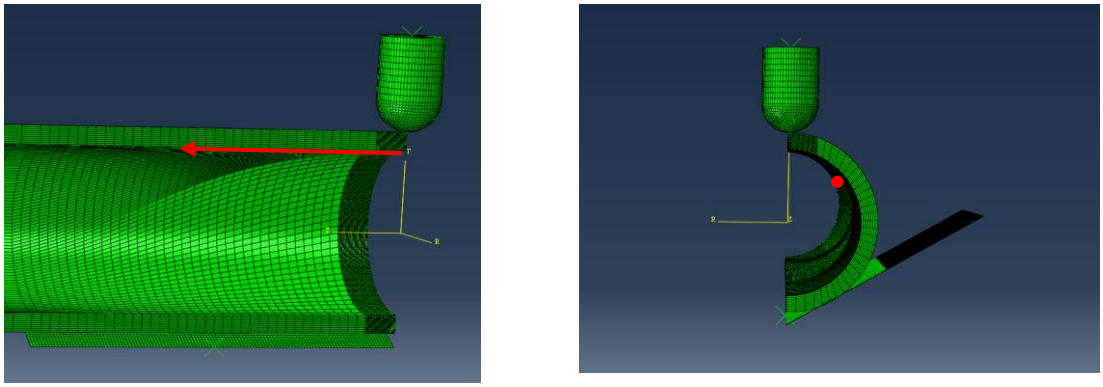

Figure 17. Simulated of a 32x2.9mm pipe during PLT condition (8% deflection of OD); arrow indicates inner fibre position.

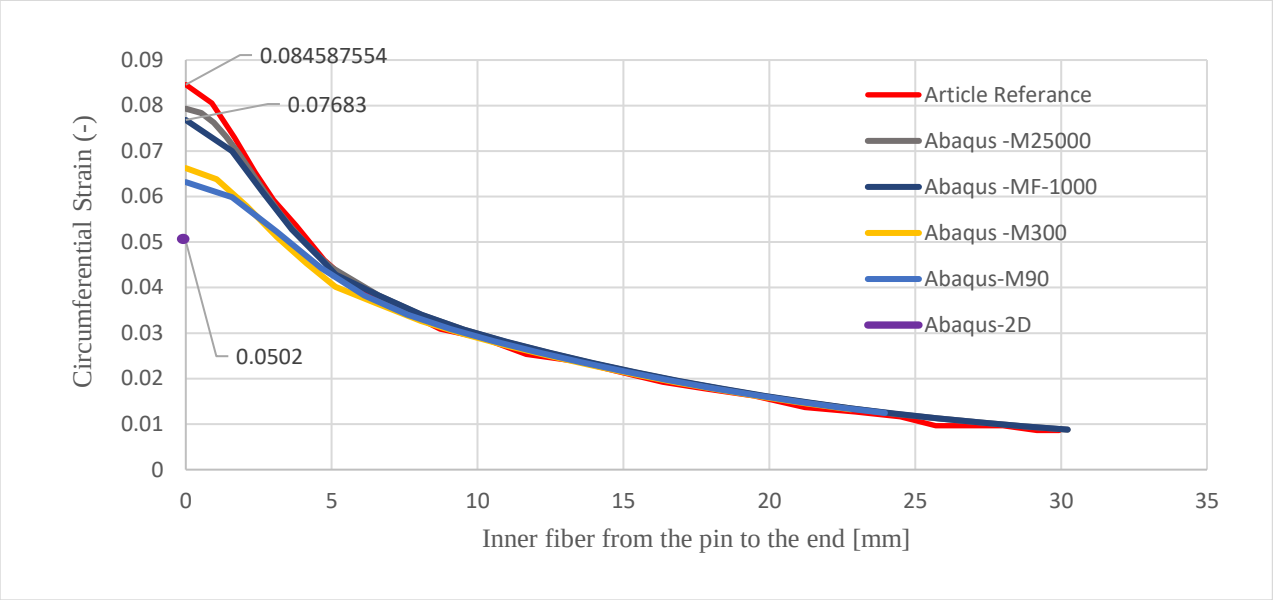

Figure 18. Circumferential strain computed along the inner fiber of the pipe wall starting below pin position

The inadequacy of the 2D model for the punching case can be attributed to its inability to capture the complex three-dimensional stress distribution around the punch. Significant out-of-plane stresses and deformations arise during punching, which a 2D model cannot accurately represent. In contrast, the 3D model effectively captures these complexities, results in better agreement with the reference results.

In the 3D case, we observed that refining the mesh improved the results towards the reference values. However, we also noted that beyond a certain level of mesh refinement, the results did not change significantly, indicating mesh convergence. This effect is illustrated in the figure 19. Therefore, there exists an optimal mesh size for the model, which we refined primarily around the point of punching.

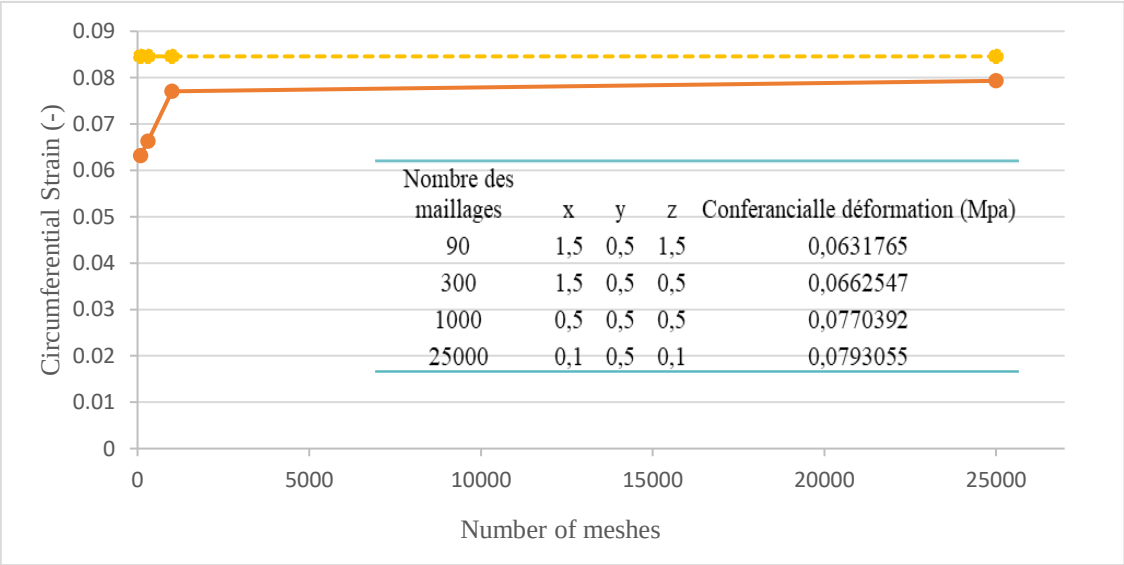

Figure 19.the effect of convergence the mesh

Additionally, the observation of mesh convergence underscores an important aspect of finite element analysis. While refining the mesh can enhance accuracy, there is a point of diminishing returns where further refinement does not significantly alter the results. Understanding this convergence behavior is crucial for conducting efficient and reliable finite element simulations.

We also found that by adjusting certain parameters, we could improve our results. For instance, using the "Not Allow Separation" option in combination with "Hard Contact Normal Behavior" ensured that the contact surfaces, once engaged, did not separate during the analysis. This setting is particularly important in simulations where a permanent bond is needed, such as with a pin inserted into a pipe where separation must be avoided once contact is established.

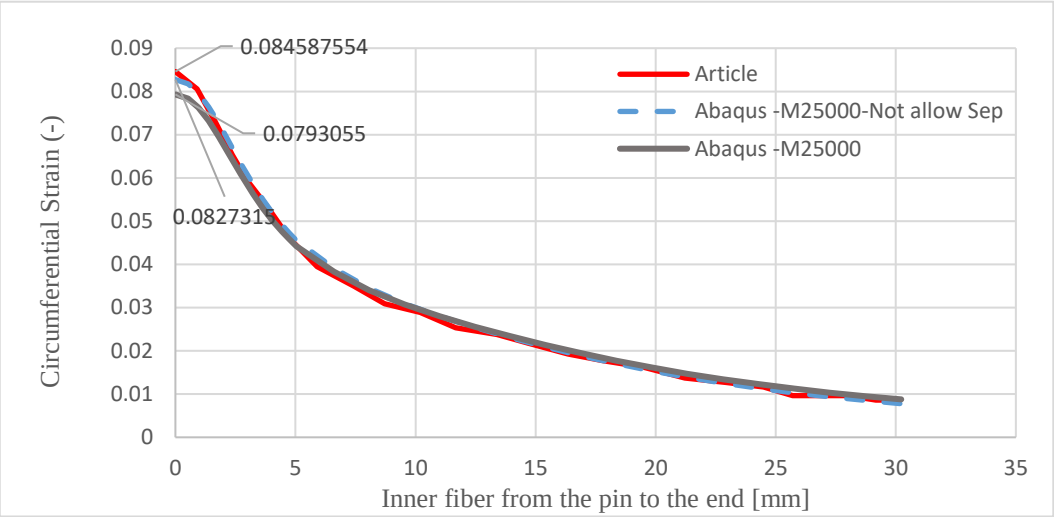

Figure 20.the effect of Not Allow Separation in the results

In table 4. you can see the parameter that we chose for the following steps:

Category	Parameter	Value
Geometry	Pipe	32 x 2.9 mm (SDR11)
	Pin Size	10 mm (Standard 1075 PLT)
	Support	60 mm with angle 120°
Material	Type	PE100
	Elastic Modulus (E)	950 MPa (20°C)
	Poisson's Ratio (ϑ)	0.35
Interaction	Contact Type	Surface to surface contact
	Normal Behavior	Hard contact, no separation
	Tangential Behavior	Penalty, friction 0.3
Load	Depth of Indentation	8% of D_ext
	Displacement for the Dent (U_y)	-2.56 mm
Mesh	Mesh Size Distribution	Biased, high accuracy near the dent

Table1. Parameters used in the 3D PLT model

Adding Thermal and Pressure Loads: According to the referenced article, the Young's modulus (E) for the material in question changes from 950 MPa at 20°C to 300 MPa at 80°C. Despite this adjustment, our observations indicated that circumferential deformation did not significantly change, as illustrated in Figure 21.

The initial observation that circumferential deformation remained unchanged suggests the need to consider other deformation modes to accurately capture the material behavior under thermal loads. Recognizing that mechanical deformation encompasses both mechanical and thermal components, we included thermal deformation in our analysis. This inclusion proved crucial, as it resulted in a deformation change of at least 20 %, demonstrating that thermal deformation is a significant factor. The referenced article and data sheet indicate that the coefficient of thermal expansion (α) for PE100 ranges between 1.3×10^{-4} K^{-1} and 5.1×10^{-4} K^{-1}, varying with temperature.

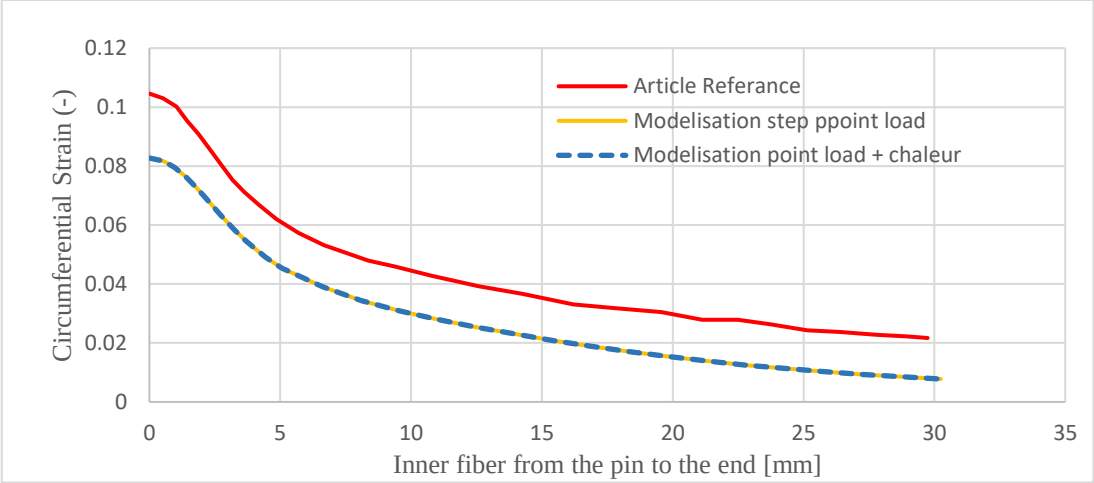

Figure21. the effect of changing young modulus in the Circumferential strain computed along the inner fiber of the pipe wall starting below pin position after heating until 80°C-

To address the impact of the coefficient of thermal expansion and to determine the appropriate value used in the referenced article for the subsequent validation steps, we conducted a parametric study. Ultimately, we found that a value of 1.5 yielded nearly perfect results. However, from the results, we can conclude that for a more realistic scenario, it is preferable to account for the temperature dependence of the coefficient of thermal expansion. Figure 22 demonstrates the impact of the coefficient of thermal expansion as reported in various studies.

The variability of the coefficient of thermal expansion with temperature further complicates the analysis. As temperature increases, the coefficient of thermal expansion increases, leading to an augmentation in the overall thermal deformation. This nuanced understanding is crucial because it underscores the importance of incorporating temperature-dependent material properties into finite element models to achieve accurate predictions.

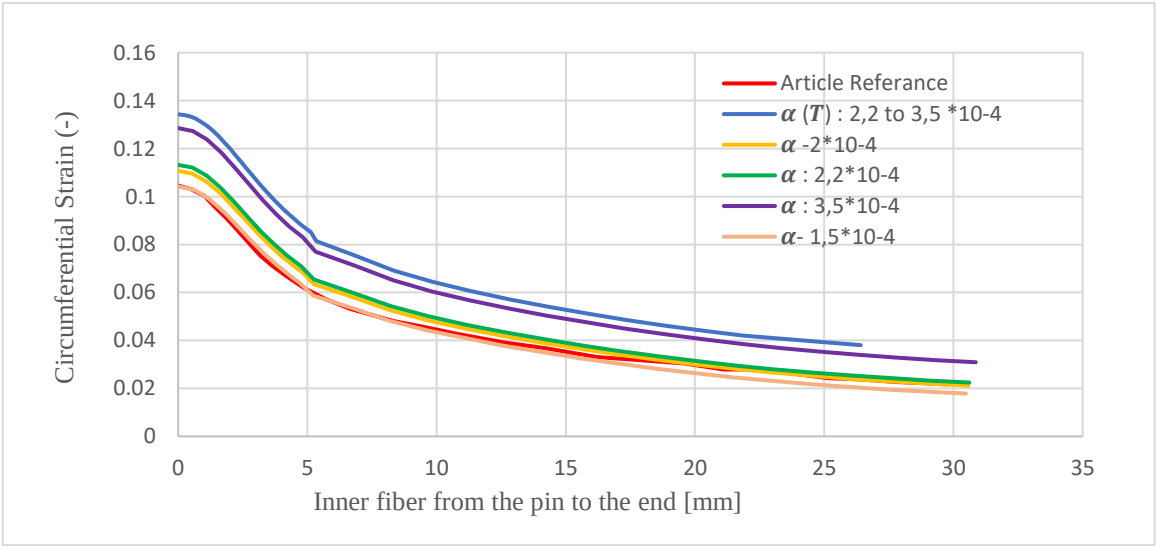

Figure22. The effect of the thermal expansion coefficient in the Circumferential strain computed along the inner fiber of the pipe wall starting below pin position after heating until 80°C

From the preceding steps, we selected a coefficient of thermal expansion of 1.5×10^{-4} K^{-1}. We then added 0.885 bar of pressure on the internal walls of the pipe and observed that the variation of the Young's modulus, which depends on temperature, plays a crucial role in our calculations. When a point load is applied with an imposed displacement, the Young's modulus does not significantly affect the circumferential deformation because the resulting deformation is primarily controlled by the imposed displacement, regardless of the material's stiffness.

However, when internal pressure is added, the Young's modulus becomes important in changing the strain. Under internal pressure, the material's response depends on its elastic properties, particularly the Young's modulus. A temperature-dependent Young's modulus directly affects the material's stiffness and hence its ability to resist deformation under an applied load. This means that different deformations will occur under the same pressure, depending on the temperature. Figure23. illustrate how the changing of the young modules affect in this step.

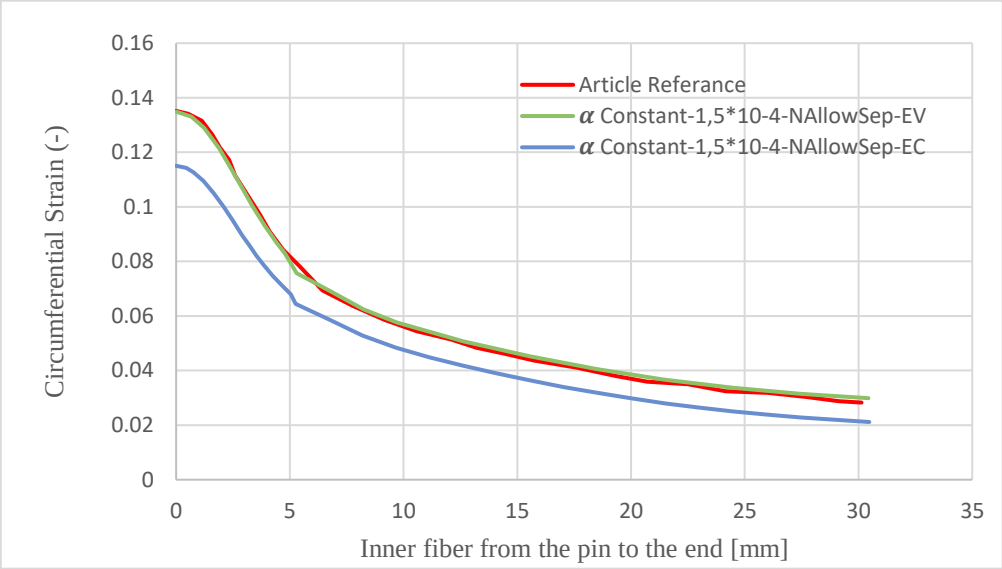

Figure23. *The effect of the changes of young modulus in function de temperature in the Circumferential strain computed along the inner fiber of the pipe wall starting below pin position after heating until 80°C and adding internal pressure.*

Adding internal pressure highlights the importance of the Young's modulus, especially when it varies with temperature. For materials subjected to simultaneous thermal and mechanical loads, it is essential to consider how their mechanical properties, such as the Young's modulus, change with temperature. The results show that for accurate and realistic simulations, it is crucial to model the Young's modulus as a function of temperature. Ignoring this variation can lead to significant errors in predicting deformations and stresses under varied thermal and mechanical conditions.

Considering the variability of mechanical properties with temperature allows for better prediction of the behavior of structures under complex loads, ensuring their reliability and safety.

Elasto-Plastic Modeling: Using the tensile test data for PE100, we processed the information to perform our analysis in Abaqus for each model, as illustrated in the corresponding figures. We considered three cases: perfect plasticity with a yield strength of 27 MPa, linear plasticity modeled by selecting two points on the stress-strain curve, and a more realistic model by intelligently choosing data points to approximate the material's actual behavior, Figuer24.

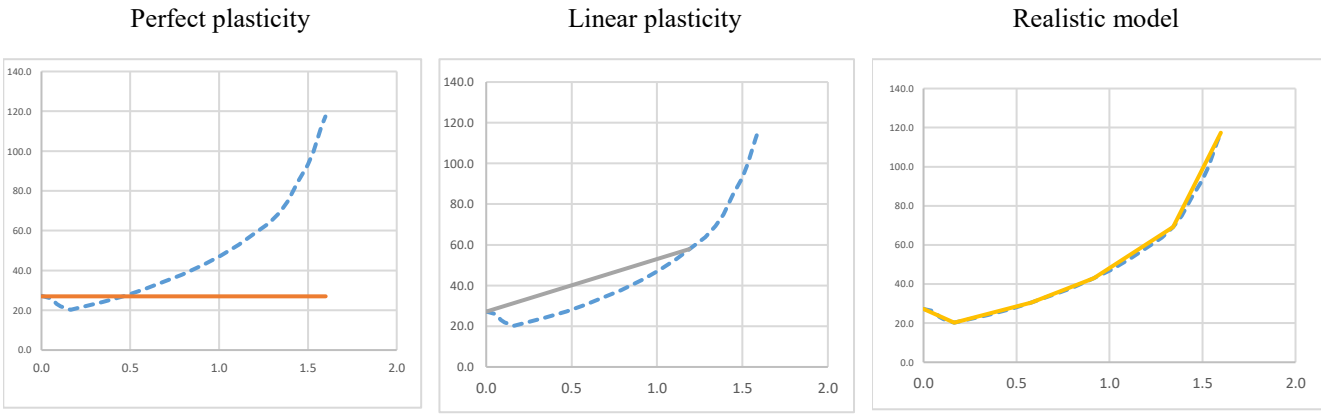

Figure24. Different model elasticity that applied in simulation

The results of our simulations are presented below figure 25. There are three different curves, each corresponding to a specific case. The curve corresponding to perfect plasticity with a threshold of 27 MPa shows a simple model to simulate but is less

realistic. The linear plasticity curve has a different shape from the other curves, with no peak. The real case curve, plotted on this graph, shows that although the behavior is similar to that of perfect plasticity, the values are very different. Therefore, it is preferable to choose the most realistic model to obtain results close to reality, even if the calculation time increases.

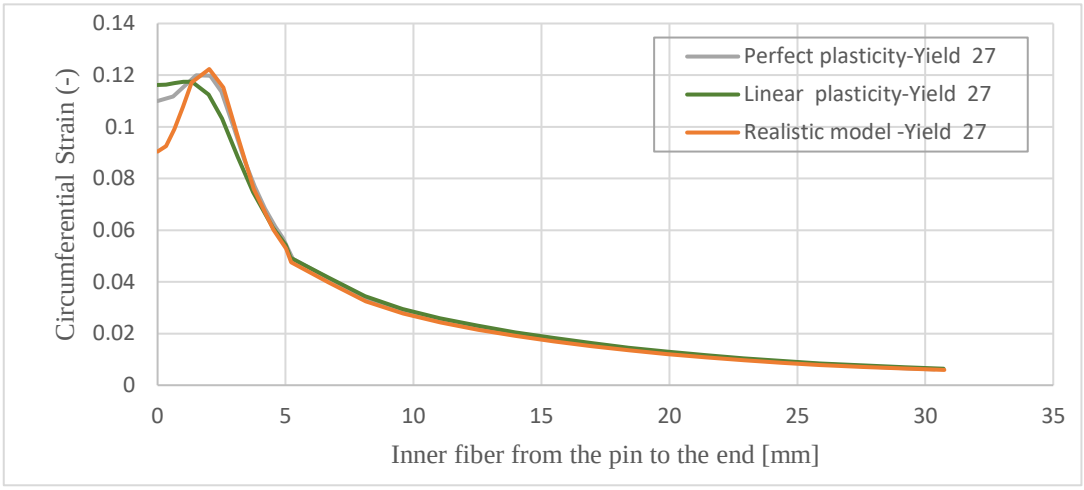

Figure 25. The effect of the different hardening model in the Circumferential strain computed along the inner fiber of the pipe wall starting below pin position after heating until 80°C

We then compared our results with those from the reference article. Figurs26. As observed, the curve with a 27 MPa yield strength did not match the reference article's results. However, by using a higher yield strength of 35 MPa and a perfect plasticity model, we obtained a curve that closely aligns with the reference data in both the point load and point load + heating scenarios. Despite this, it should be noted that this does not represent a real-world case.

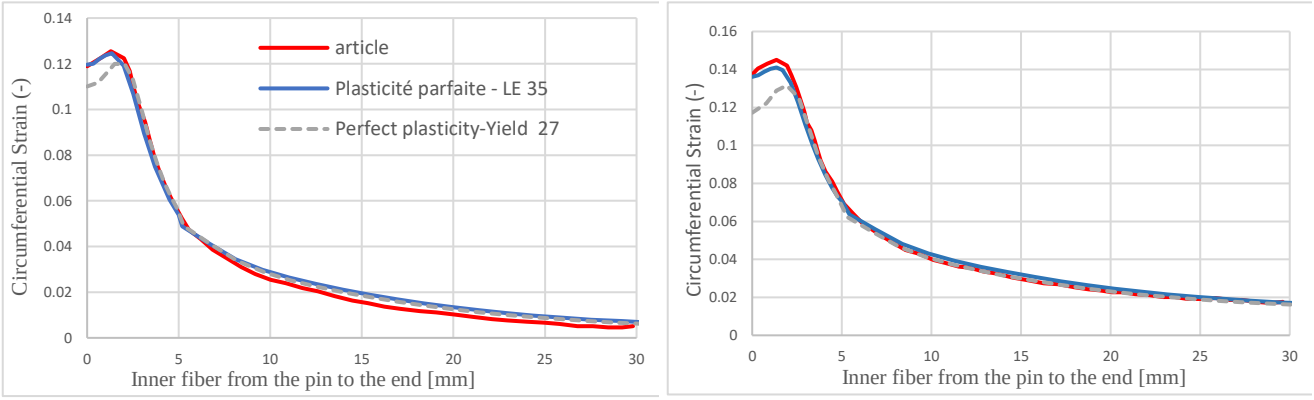

Figurs26. Circumferential strain computed along the inner fiber of the pipe wall starting below pin position in PLT scenario (left) and PLT + Heating Scenario(Right)

Subsequently, we introduced internal pressure and observed that with the adjusted yield strength, the results improved. A parametric study was conducted by varying the yield strength and temperature (80°C). As depicted in the figure, increasing the yield strength initially causes deformation to increase, and the peak of the curve shifts to the left, indicating a reduction in the plastic zone. However, beyond a certain value, further increasing the yield strength at 80°C results in a decrease in total deformation. Figure27.

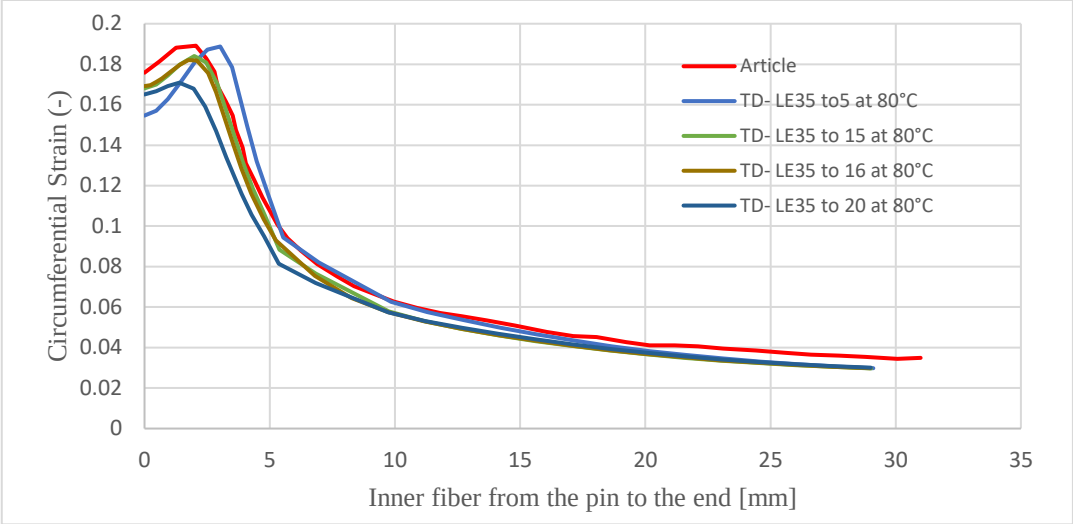

Figure 27. Parametric Study on the Variation of Yield Strength at 80°C

4.2. PHASE 2: CHEMICAL DEGRADATION ASSESSMENT: EFFECTS OF CHLORINE DISINFECTION

In this section, we present the results of various tests conducted to assess the mechanical and physico-chemical properties of HDPE, specifically PE100. The objective was to analyze these properties both before and after degradation due to chlorine exposure. However, due to the extensive time required for aging on the platform provided by SUEZ, only the results before aging will be presented at this time.

Additionally, we have included results on the mechanical and physico-chemical behavior of the material after film fabrication. The results are structured as follows:

Firstly, we present the mechanical behavior of HDPE using simple uniaxial traction tests in three states: the sample of the pipe in its original form, samples fabricated from a film with a thickness of 600 microns at ambient temperature, and the mechanical behavior of the film at 40°C.

Following this, we will detail the chemical characterization using thermogravimetric analysis (TGA), Fourier transform infrared spectrometry (FTIR), differential scanning calorimetry (DSC), and oxidative induction time (OIT).

Mechanical characterization: uniaxial tensile tests

Our study focused on determining the Young's modulus, elastic limit, and elongation at break of the materials. Tests were conducted under controlled conditions of 23°C and 50% humidity, using different test speeds: 10 mm/min for thicker specimens and 5 mm/min for films with a thickness less than 1 mm. For tests conducted at 40°C, the films were tested at the same speed of 5 mm/min. Once the raw stress-strain curve is obtained, which shows the variation in load (F) applied to the specimen as a function of the elongation (ΔL) it undergoes, it is necessary to normalize this curve to eliminate the influence of the initial dimensions of the specimen and to focus solely on the material's properties.

To achieve this, we divide the load (F) by the initial cross-sectional area (S_0) of the specimen to obtain the nominal stress (σ). The vertical axis is then scaled in stress units (MPa). Similarly, we divide the elongation (ΔL), which is the difference between the instantaneous length (L) and the initial length (L_0), by the initial length (L_0). This gives us the strain, typically expressed as a percentage (%), and the horizontal axis becomes the strain axis (ε). This normalized curve is referred to as the nominal tensile stress-strain curve or simply the tensile curve.

However, for inputting material properties into Abaqus, we require true stress and true strain curves. Therefore, further data processing is necessary. To obtain the true stress (σ_{true}) and true strain (ε_{true}) required for more accurate analysis, we use the following transformations:

$$\sigma_{true} = \sigma\,(1+\varepsilon) \qquad \textit{Eq.9}$$

$$\varepsilon_{true} = Ln\,(1+\varepsilon) \qquad \textit{Eq.10}$$

These calculations ensure that the stress-strain data accounts for the continuous deformation and actual material behavior during testing, providing a more precise representation of the material's response under load.

In Figure 28, I will present the results obtained for PE100 in both pipe and film forms with varying thicknesses. It is evident that samples fabricated from the film using the compression press method at 180°C and 160°C exhibit nearly identical mechanical properties. This observation allows us to conclude that reheating the material to a molten state and then fabricating the film does not significantly alter its mechanical properties.

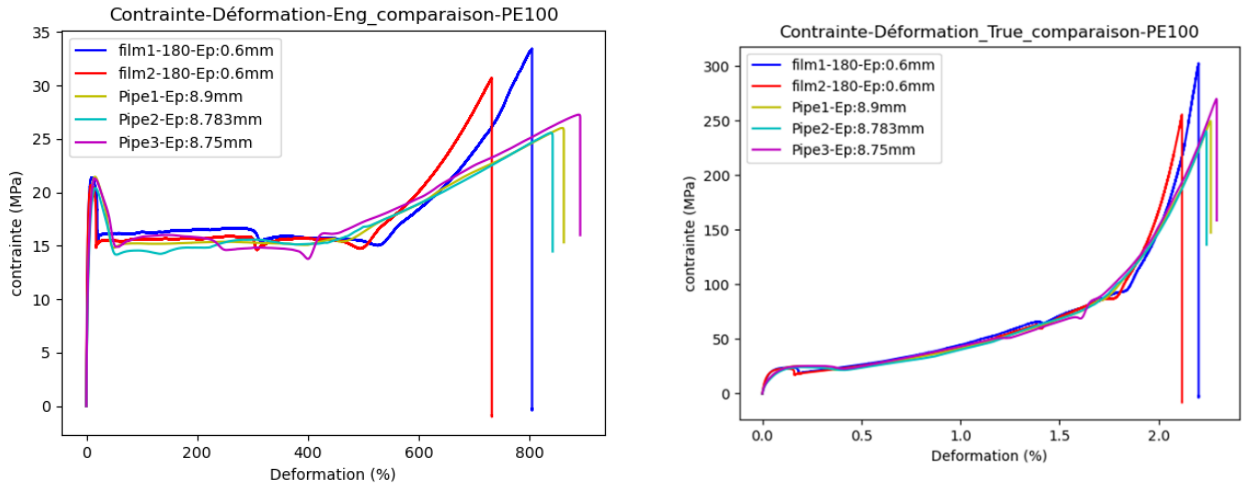

Figure 28. Results of the Tensile Test for PE100: Nominal Stress-Strain Curve (left) and True Stress-Strain Curve (right)

In the figure29. you can observe the properties of PE100 at 40°C. However, due to equipment limitations within the oven, measurements for elongation at yield and yield strength were not possible. Nevertheless, we have captured the material's behavior within the plastic range, which is essential for inputting data into Abaqus.

In the table.5. all the mechanical properties information is shown. Some information for the test at 40 °C is missing due to machine limitations (limited imposed displacement).

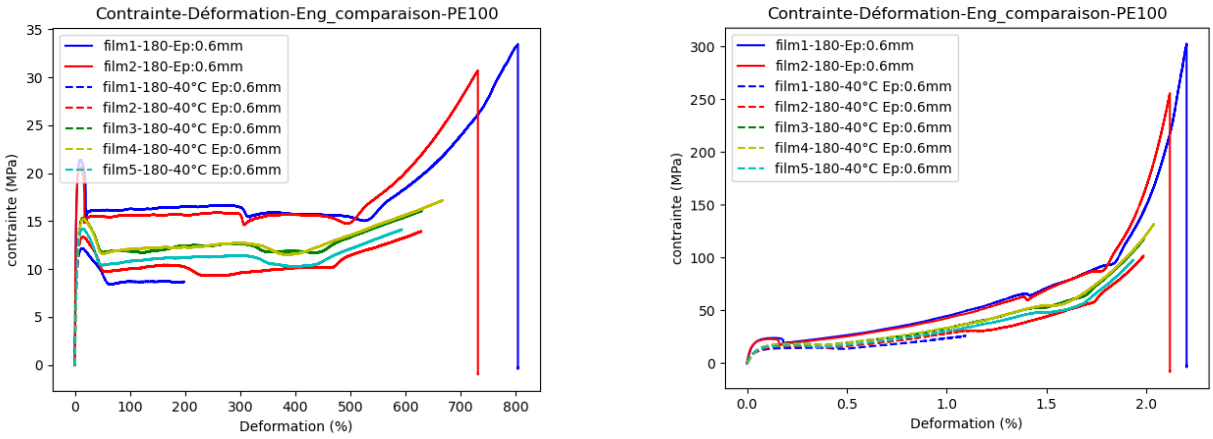

Figure 29. Results of the Tensile Test for PE100 at 40°C: Nominal Stress-Strain Curve (left) and True Stress-Strain Curve (right)

Exposure time: **0 Day**				
Semple	Young's Modulus	Elongation at Break	Yield Strength	Tensile Strength
	(MPa)	**(%)**	**(MPa)**	**(MPa)**
PE100-Pipe -001	751,3	861,4	21,45	26,03
PE100-Pipe -002	668,0	841,3	20,40	25,58

PE100-Pipe -003	757,2	890,9	21,27	27,28
PE100-Film-180°C-001 (at 23°C)	782,4	1004,8	20,00	33,11
PE100-Film-180°C -002 (at 23°C)	772,6	1493,0	20,60	30,61
PE100-Film-180°C -003 (at 40°C)	511,5		12,1	
PE100-Film-180°C -004 (at 40°C)	490,8		13,3	
PE100-Film-180°C -005 (at 40°C)	460,9		15,3	
PE100-Film-180°C -006 (at 40°C)	331,3		15,3	
PE100-Film-180°C -007 (at 40°C)	489,4		14,2	

Table5. the mechanical properties of PE100

ATG Results

Thermogravimetric analysis (TGA) is a thermal technique well-suited for assessing the stability of polymeric materials. Under high temperatures, polymers decompose, resulting in the formation of various low molecular weight products. TGA provides valuable insights into the behavior of polymers during oxidation or thermal degradation, offering predictive data for their performance under real atmospheric conditions. In this experiment, we anticipate that TGA results will reveal structural changes due to degradation from chlorine disinfectant exposure.

The thermal stability of PE100 composites was initially investigated using TGA under a nitrogen atmosphere with a heating rate of 20°C/min. The analysis revealed that the decomposition of HDPE-PE100 composites occurs in two distinct steps (Table 6). The first decomposition step occurs approximately between 485°C and 490°C, corresponding to the degradation of Polymer part. The second degradation step, around 615°C to 625°C, is attributed to the degradation of HDPE carbon black. The residual mass after polymer degradation was found to be approximately 1.8% of the initial mass, indicating that the carbon black content in PE100 is 1.8% of the initial mass, while the remaining 98.2% consists of polymer and antioxidants. Table 6 summarizes the temperatures of polymer and carbon black degradation, along with the corresponding mass percentages before and after film fabrication of PE100, providing crucial data for the ATG section of my report.

Exposure time: 0 Day				
specimens	**PE100-Film-180°C-001**	**PE100-Film-160°C-001**	**PE100-Film-160°C-002**	**PE100-Pipe-001**
Temp _Deg of polymer (°C)	491,9	489,7	490,3	485,8
Temp _Deg of carbon black (°C)	616,6	624,2	622,3	620,6
% Mass of Polymer	98, 2%	98,2%	98,1%	98,2%
% Mass of carbon black	1,8%	1,8%	1,9%	1,8%

Table 6. the result of the temperatures of polymer and carbon black degradation

FTIR spectroscopy results

In this section, I will present the results of the experimental characterization, specifically focusing on the FTIR spectroscopy results. As previously explained, we characterized the materials at different stages. Initially, we characterized the materials in their non-aging and virgin stages (PE100). Once we manufactured the films under high temperature (180°C) and pressure, we performed another round of characterization to ensure that these conditions did not alter the properties of the materials. Therefore, all the data presented here are before and after the fabrication of...

Figures30. depict the transmittance spectra of infrared waves for the samples before and after film production. These spectra will be analyzed to interpret any changes in the chemical structure of the materials throughout the fabrication process.

The observed peaks at 2914, 2847, 1743, 1461, and 716 cm^{-1} can be interpreted as follows:

- Peaks at 2914 cm^{-1} and 2847 cm^{-1} indicate C-H stretching vibrations, confirming the presence of methylene groups characteristic of polyethylene.
- A peak at 1743 cm^{-1} suggests the presence of carbonyl groups, indicative of some oxidation, possibly due to environmental exposure.
- The peak at 1461 cm^{-1} corresponds to CH2 bending vibrations, further confirming the polyethylene structure.
- The peak at 716 cm^{-1} is associated with CH2 rocking vibrations, indicating the crystalline nature of the polymer.

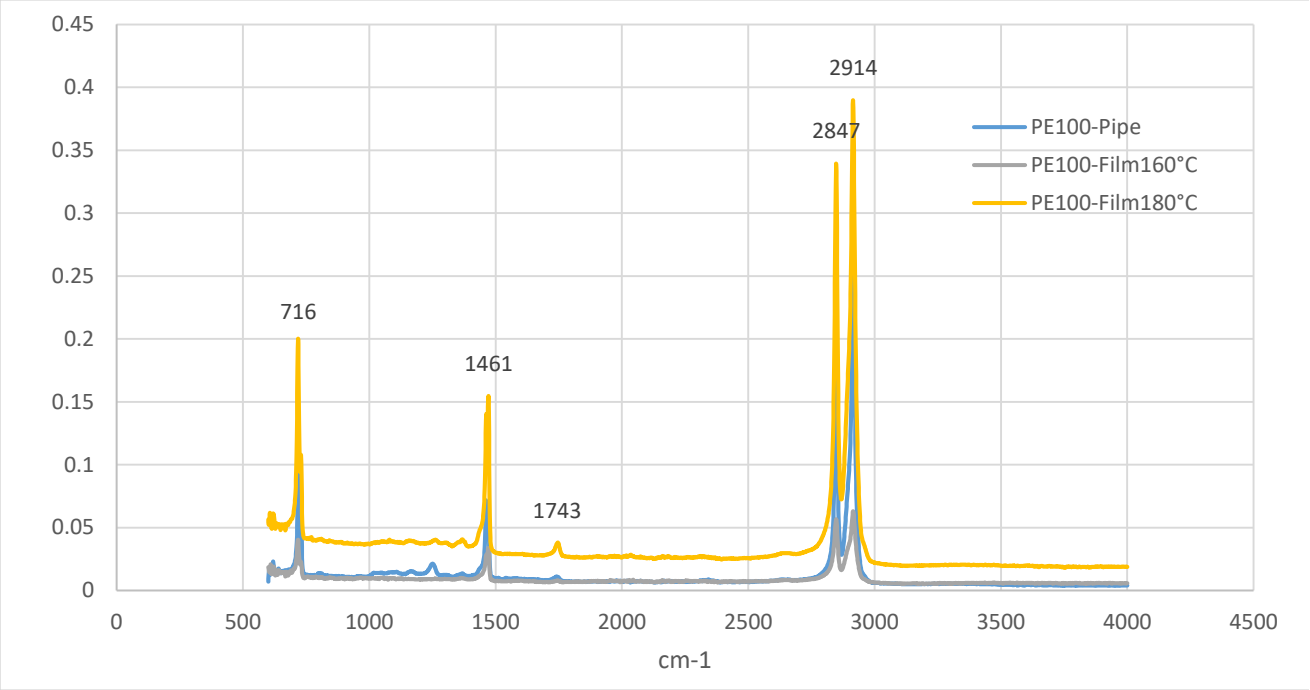

Figures30. FTIR spectroscopy results for PE100 before and after film fabrication

DSC Results

DSC measurements were conducted to monitor changes in the crystallinity of HDPE pipes before and after film fabrication at temperatures of 180°C and 160°C. This was important due to the known effect that structural changes, induced by fabrication or degradation, can have on material properties. From the results presented in Table 7, it is evident that the melting temperatures and crystallinity rates were recorded.

Across all samples, there was no significant variation in melting temperatures. However, a slight difference in crystallinity rates was observed specifically in the samples fabricated at 160°C. It is hypothesized that the rapid cooling method used may have influenced these crystallinity rates.

Exposure time: 0 Day				
PE100	Specimens 1	Specimens 2	Specimens 3	Moyenne
T_Melting	129,8	129,9	129,3	129,7
crystallinity rates	63,2%	64,6%	64,4%	64,1%
PE100- Film-180°C -Slow cooling				
T_Melting	129,5	129,8	129,6	129,7
crystallinity rates	61,2%	60,7%	61,4%	61,1%
PE100- Film-160°C-Rapid Cooling				
T_Melting	127,9	128,3		128,1
crystallinity rates	57,2%	57,3%		57,3%
PE100- Film-160°C - Slow cooling				
T_Melting	128.7	129.7		129.2
crystallinity rates	61.4	63.3		62.35

Table 7. Result of DSC test for PE100 in different condition

Conversely, for the PE films fabricated at 160°C with a slow cooling process, the crystallinity rate increased and closely matched that of the original PE100 pipe before film fabrication.

OIT Results

This section presents the results of the Oxidative Induction Time (OIT) tests conducted using two different methods. In the first method, the material was heated to 220°C, and in the second method, it was heated to 200°C. All results are summarized

in Table 8. As shown, the OIT values increase as the temperature decreases. This observation aligns with the Arrhenius law, which states that the reaction rate decreases with a reduction in temperature. Consequently, the rate of oxidation slows down at lower temperatures, resulting in higher OIT values.

these results indicate that the oxidative stability of the material improves at lower temperatures. The increase in OIT with decreasing temperature suggests that the material is less prone to oxidation and degradation under lower thermal conditions. This behavior is crucial for applications where long-term thermal stability is required, such as in piping systems exposed to varying environmental conditions.

The variation in oxidation rates with temperature also provides valuable insights for predicting the material's performance and lifespan. By understanding the temperature dependence of oxidation, we can better assess the durability and reliability of HDPE pipes and films in real-world applications.

Exposure time: 0 Day				
Samples	**mass**	**Test temperature**	**OIT**	**The oxidation rate**
	(mg)	(°C)	(min)	(W/g.min)
PE100-Film160°C-001	5.07	220	21.3	1.
PE100-Film180°C-001	5.39	220	19.5	0.7
PE100-Pipe-001	7.94	220	22.4	0.7
PE100-Pipe-002	6.24	220	23.0	0.9
PE100-Pipe-003	8.88	200	122.7	0.1
PE100-Pipe-004	8.16	200	121.0	0.1
PE100-Pipe-005	7.35	200	116.5	0.1

Table8. The results of OIT for the PE100 in different condition

5. Concluding Remarks

The research undertaken during this internship involved a comprehensive analysis of the performance and lifetime of PE100 pipes, particularly under the combined effects of mechanical punching and chemical degradation. Before this, it was crucial to validate our modeling with a reference case to ensure that the chosen parameters were optimal among the many options available in Abaqus. Therefore, the first step was to validate our model by simulating a case from an existing article and then comparing the results with those in the article.

In this purpose, Abaqus Finite Element software was utilized to simulate the mechanical stresses and strains in PE100 pipes under various conditions. A quarter of a 3D model of the pipe, the pin and the counter support were simulated in three sequence steps (Punching + Heating + Pressure intern). In this part of the project, we understood that when an imposed displacement is applied, the value of Young's modulus is not as crucial as when an imposed force is applied. Additionally, in the case of point load, it is not feasible to reduce our model to a 2D case due to the inability to capture the complex three-dimensional stress distribution around the punch. Significant out-of-plane stresses and deformations arise during punching, which a 2D model cannot accurately represent. In contrast, the 3D model effectively captures these complexities, resulting in better agreement with the reference results.

It was also observed that thermal deformation can be as significant as mechanical deformation when the pipe operates at high temperatures. In the case of punching load and heating, without considering the coefficient of thermal expansion, the results remain unchanged. However, when including the change in Young's modulus as a function of temperature, the deformation under the pin shows significant variation. The initial value at zero point is 0.81, and after adding the coefficient of thermal expansion, the value changes to 0.1, indicating that the deformation altered by more than 20%.

In the case of elasto-plastic behavior, it was also observed that when adding the plasticity model, the change in deformation is not linear as in the elastic case. The variation in deformation is significantly different depending on the yield limit value, not only at ambient temperature but also at 80°C.

The study compared three plasticity models: perfect plasticity, linear plasticity, and a model approximating real material behavior. It was evident that the perfect plasticity model, despite its simplicity, fails to capture the nuances of material deformation under stress. The linear plasticity model, although closer to reality, still diverged significantly from actual

behavior. The most realistic model, which involves strategically selecting data points, provided the most accurate representation, albeit with higher computational costs.

Additionally, in the case of PL + heating + internal pressure, it was observed that when adding the plasticity model, the change in deformation is not linear as in the elastic case. The deformation varies significantly depending on the yield limit value, not only at ambient temperature but also at 80°C.

In the second phase of the project, we would investigate the chemical degradation of polymer pipes exposed to chlorinated disinfectants commonly used in drinking water treatment. Based on articles, we predicte that changes in the number of chains and, consequently, molecular weight caused by chain scissions can significantly alter the physical and mechanical properties of PE pipes. However, since we do not yet have the aging materials for the tests, we cannot present any results in this report. The aging tests were initiated on May 26, and we do not yet have the specimens after one month of aging to observe this effect.

Thus, we only have results for the virgin material. In the investigation of the mechanical properties of PE100, it was observed that the properties of the material for the film fabricated at 180°C or at 160°C do not change significantly. However, the cooling rate in the process of fabrication of the film can impact the crystallinity of the material. Rapid cooling results in a slightly lower crystallinity rate. therefore, consequently its mechanical properties will change.

With doing the tensile test at tow temperature we observed that, the properties of the material at 40°C during the tensile test change drastically. For example, the Young's modulus at 23°C is on average 746 MPa, while at 40°C it drops to 456 MPa, representing a decrease of up to 40%. The yield strength also decreases from 21 MPa to 14 MPa, a change of 32%.

Finally, the section concludes with a consideration of lifetime prediction, specifically focusing on the combined influence of punching and chemical degradation in polymer pipes. The literature review highlights the gaps in assessing the lifetime of polymer pipes, specifically HDPE, concerning the combination of two phenomena: punching caused by external load and chemical decay due to chlorine disinfectants in water systems.

As the third phase of the project depends on the data from phase two and the results after degradation, we are currently unable to proceed with this phase

Moreover, while our comparisons thus far have been primarily visual, it is imperative to enhance precision and reliability through analytical comparisons in future studies. Refining computational models to integrate intricate degradation mechanisms and their interactions is essential.

Our study proposes the use of computational models and chemical assessments for a detailed analysis. The goal is to understand the mechanical stresses from different PL parameters and estimate pipe lifetime, considering both mechanical and chemical degradation. This approach is crucial for developing predictive models and maintenance strategies, ultimately extending the lifetime of polymer pipes in water distribution systems.

References

A. Boujlal, Analysis Of Slow Crack Initiation Of Old Polyethylene Resins By Means Of An Elasto-Visco-Plastic Rheological Model: Experimental And Numerical Approach, *Plastic Pipes XVI*, Barcelona, Spain, 2012

A. Frank, "A numerical methodology for lifetime estimation of HDPE pressure pipes", *Engineering Fracture Mechanics*, 78, 2011, p. 3049–3058.

A. Frank, G. Pinter, R.W. Lang, "Prediction of the remaining lifetime of polyethylene pipes after up to 30 years in use", *Polymer Testing* 28, 2009, p. 737–745.

A. Sukhadia, "Assessing the Slow Crack Growth Resistance of PE Resins and Pipe Service Lifetimes Predictions", *15th Plastic Pipes conference, PPXV*, Vancouver, Canada, 2010.

A. Tripath, S. Mantell, J. Le, "Chemo-mechanical modeling of static fatigue of high density polyethylene in bleach solution", *International Journal of Solids and Structures*, 217–218, 202, p. 90–105.

ASTM D2837, "Standard Test Method for Obtaining Hydrostatic Design Basis for Thermoplastic Pipe Materials or Pressure Design Basis for Thermoplastic Pipe Products", ASTM D2837, ASTM International, West Conshohocken, 2013.

B.-H. Choi, A. Chudnovsky, R. Paradkar, W. Michie, Z. Zhou, P.-M. Cham, "Surface degradation of HDPE-100 pipe: Effects of some aggressive environments (solvents) ", *Polymer Degradation and Stability*, 94 (5), 2009, p. 859–867 May 2009.

B. Fayolle, X. Colin, L. Audouin, J. Verdu, "Mechanism of degradation induced embrittlement in polyethylene", *Science Direct Polymer Degradation and Stability*, 92, 2007, p. 231-238.

DIN EN ISO 9080, "Plastics piping and ducting systems –Determination of the long-term hydrostatic strength of thermoplastics materials in pipe form by extrapolation", 2003.

Dossier technique conduit 9010 RC en PE 100-RC.

E. Van Der Stok, F. Scholten, "Two complementary tests to determine the quality of pe 100-RC", *17th Plastic Pipes Conference PPXVII*, Chicago, Illinois, USA, 2014.

E.M. Hoang, D. Lowe, "Lifetime prediction of a blue PE100 water pipe", *Polymer Degradation and Stability*, 93(8), 2008, p. 1496.

F.L. Scholten, D. Gueugnaut, F. Berthier, "A More Reliable Detergent for Cone and Full Notch Creep Testing of PE Pipe Materials", *11th Plastic Pipes conferences, PPXI*, Munich,Germany, 2001.

H. Bromstrup, PE 100 pipe systems, 2nd edition, 2004, p. 15- 35.

ISO 13480, "Polyethylene pipes - Resistance to slow crack growth - Cone test method", 1997.

ISO 9080, Plastics Piping and Ducting Systems, "Determination of the Long-term Hydrostatic Strength of Thermoplastics Materials in Pipe Form by Extrapolation", ISO 9080, CEN, Brussels, 2003.

J. Hassinen, M. Lundbäck, M. Ifwarson, U.W. Gedde, "Deterioration of polyethylene pipes exposed to chlorinated water", *Polymer Degradation Stability*, 84(2), 2004, p.261-267.

J. Hessel, "Minimum service-life of buried polyethylene pipes without sand embedding", *3R international Special Plastics Pipes*, 40(6), 2001, p. 178-184.

J. Lenz, "Long-Term Point Loads Testing with Plastic Pipes", *11th plastic pipe conference, PPXI*, Munich, Germany, 2001.

L. Andena, M. Rink, R. Frassine, and R. Corrieri, "A fracture mechanics approach for the prediction of the failure time of polybutene pipes", *Engineering Fracture Mechanics*, 76(18), 2009, p. 2666-2677.

M. Farshad, "Two new criteria for the service life prediction of plastics pipes", *Polymer Testing*, 23(8), 2004, p. 967-972.

M. Haager, "Fracture mechanics methods for the accelerated characterization of the slow crack growth behavior of polyethylene pipe materials", *Doctoral Dissertation, Institute of Materials Science and Testing of Plastics*, University of Leoben, Austria, 2006.

N. Brown, X. Lu, “Controlling the Quality of PE Gas Piping Systems by Controlling the Quality of the Resin”, *Proceedings of the 13th Plastic Fuel Gas Pipe Symposium*, San Antonio, Texas, USA, 1993.

N. Brown, X. Lu, “PENT quality control test for PE gas pipes and resins”, *Proceedings of the 12th Plastic Fuel Gas Pipe Symposium*, Boston, Massachusetts, USA, 1991.

P. Hutař, M. Ševčík, L. Náhlík, G. Pinter, G. Pluvinage, M. Elwany, “Safety, Reliability and Risk Associated with Water, Oil and Gas Pipeline”, 2007.

P. Hutar, M. Sevcik, L. Nahlik, G. Pinter, A. Frank, I. Mitev, “A numerical methodology for lifetime estimation of HDPE pressure pipes”, *Engineering Fracture Mechanics*, 78(17), 2011, p. 3049-3058P.

P. Hutar, M. Ševcík, A. Frank, L. Náhlík, J. Kucera, and G. Pinter, “The Effect of Specimen Size on the Determination of Residual Stress in Polymer Pipe Wall”, Engineering Fracture Mechanics, 108, 2013, p. 98.PAS1075:2009-04, “Pipes made from Polyethylene for alternative installation techniques – Dimensions, technical requirements and testing”, 2009-04.

Plastics Pipe Institute (PPI), Handbook of Polyethylene Pipe, 2nd edition,2008, p. 43-103.

S. Nestelberger, J. Cheng, “Finite element method (fem) used to simulate the stress/strain of the point load test (PLT) in a broader study to support the future iso test standard”, *Proceedings of the 20th Plastic Pipes Conference PPXX*, Amsterdam, Netherland, 2021.

U. Niebergall, O. Mertlová, E. Nezbedová, “Full Notch Creep Test - ISO Round Robin Test”, *13th Plastic Pipes conference, PPXIII*, Washington DC, USA, 2006.

V. Rouyer, M. Cornette, “Resistance of Crosslinked PE Pipes to Rock Impingement”, *Proceedings of the 11th Plastic Pipes Conference PPXI*, Munich Germany, 2001.

W. Yu, B. Azhdar, D. Andersson, T. Reitberger, J. Hassinen, T. Hjertberg, U.W. Gedde, “Deterioration of polyethylene pipes exposed to water containing chlorine dioxide”, *Polymer Degradation and Stability*, 96, 2011, p. 790-797.

X. Colin, L. Audouin, J. Verdu, M. Rozental-Evesque, B. Rabaud, F. Martin, F. Bourgine, “Aging of Polyethylene Pipes Transporting Drinking Water Disinfected by Chlorine Dioxide. I. Chemical Aspects”, *Polymer Engineering And Science*, 49(7), 2009, p. 1429-14376.

X. He, X. Zha, X. Zhu, X. Qi, B. Liu, “Effect of short chain branches distribution on fracture behavior of polyethylene pipe resins”, *Polymer Testing*, 68, 2018, p. 219-228.

X. Zheng, X. Zhang, L. Ma, W. Wang, J.g Yu, “Mechanical characterization of notched high density polyethylene (HDPE) pipe: Testing and prediction”, *International Journal of Pressure Vessels and Piping*,173, 2019, p. 11-19.

Y. Huang, Q. Zhang, X. Lu, Y. Gong, H. Zhou, J. Feng, “Comparative Investigation on Step-cycle Tensile Behaviors of Two Bimodal Pipe-grade Polyethylene with Different Slow Crack Growth Resistance”, *Chinese Journal of Polymer Science*, 38, 2020, p. 611–619.

Z. J. Zho, D. Chang, “Stress intensity effect on slow crack growth in scratched polyethylene pipe”, *15th Plastic Pipes Conference PPXV*, Vancouver, Canada, 2010.

Z. Xiong, R. Wei, “A New Point Loading Test Method For HDPE Pipe Materials”, *16th Plastic Pipes Conference*, PPXVI, Barcelona, Spain, 2012.